BRNO UNIVERSITY OF TECHNOLOGY
VYSOKÉ UČENÍ TECHNICKÉ V BRNĚ

FACULTY OF MECHANICAL ENGINEERING
FAKULTA STROJNÍHO INŽENÝRSTVÍ

INSTITUTE OF MACHINE AND INDUSTRIAL DESIGN
ÚSTAV KONSTRUOVÁNÍ

DESIGN OF NON-RESONANT SAMPLE HOLDERS
NÁVRH NE-REZONAČNÍCH DRŽÁKŮ VZORKŮ

BACHELOR'S THESIS
BAKALÁŘSKÁ PRÁCE

AUTHOR — **Adam Lagiň**
AUTOR PRÁCE

SUPERVISOR — **Ing. Antonín Sojka**
VEDOUCÍ PRÁCE

BRNO 2020

BRNO UNIVERSITY OF TECHNOLOGY
FACULTY OF MECHANICAL ENGINEERING

Specification Bachelor's Thesis

Department:	Institute of Machine and Industrial Design
Student:	**Adam Lagiň**
Study programme:	Engineering
Study branch:	Fundamentals of Mechanical Engineering
Supervisor:	**Ing. Antonín Sojka**
Academic year:	2019/20

Pursuant to Act no. 111/1998 concerning universities and the BUT study and examination rules, you have been assigned the following topic by the institute director Bachelor's Thesis:

Design of non–resonant sample holders

Concise characteristic of the task:

High field Electron Paramagnetic Resonance (HF–EPR) spectroscopy has a significant influence on the research of novel devices for quantum computation, high–capacity data storage or MW detectors. Materials for these researcher require different samples, such as press powder pellets, single crystals, nanofabricated devices on the chips, or deposited thin films. Therefore, a specific EPR sample holders are essential for multi–purpose investigations.

Type of the work: developmental – constructional

Goals Bachelor's Thesis:

The aim of this work is the design of unique non–resonant sample holders for an HF–EPR spectrometer to be used for measurements of pressed–powder pellets, necessary for studying bulk properties of molecules, and for measurements of chip devices, for studying electronic and transport properties.
Partial goals of bachelor thesis:
– description of HF–EPR spectroscopy convenient for sample holder design,
– design of non–resonant sample holders for powder–pressed pellets and chip devices,
– drawing documentation,
– realization (production, measurements).

Required outputs: drawings of parts and assemblies, accompanying report.
Range of the work: 27 000 signs (15 – 20 pages without pictures).
Schedule, structure of the work and template of the accompanying report are mandatory:
http://www.ustavkonstruovani.cz/download/Ukonceni–studia/2020_Zasady_vypracovani_VSKP.pdf

Recommended bibliography:

WEIL, John A. a James R. BOLTON. Electron paramagnetic resonance: elementary theory and practical applications. 2nd ed. Hoboken, N.J.: Wiley-Interscience, c2007. ISBN 978-0471754961.

MÖBIUS, Klaus a Anton SAVITSKY. High-field EPR spectroscopy on proteins and their model systems: characterization of transient paramagnetic states. Cambridge, UK: Royal Society of Chemistry, c2009. ISBN 08-540-4368-3.

NEUGEBAUER, Petr, Dominik BLOOS, Raphael MARX, et al. Ultra-broadband EPR spectroscopy in field and frequency domains. Physical Chemistry Chemical Physics. 2018, 20(22), 15528-15534. DOI: 10.1039/C7CP07443C. ISSN 1463-9076. Dostupné také z: http://xlink.rsc.org/?DOI=C7CP07443C

BLOOS, Dominik, Jan KUNC, Louise KAESWURM, et al. Contactless millimeter wave method for quality assessment of large area graphene. 2D Materials. 2019, 6(3). DOI: 10.1088/2053-1583/ab1d7e. ISSN 2053-1583. Dostupné také z: https://iopscience.iop.org/article/10.1088/2053-1583/ab1d7e

SHIGLEY, Joseph Edward, Charles R MISCHKE a Richard G BUDYNAS. Konstruování strojních součástí. Brno: VUTIUM, 2010. Překlady vysokoškolských učebnic. ISBN 978-80-214-2629-0.

Deadline for submission Bachelor's Thesis is given by the Schedule of the Academic year 2019/20

In Brno,

L. S.

prof. Ing. Martin Hartl, Ph.D. Director of the Institute	doc. Ing. Jaroslav Katolický, Ph.D. FME dean

ABSTRAKT

Paramagnetické látky a nano-elektrické zariadenia môžu nájsť uplatnenie pri vývoji kvantových počítačov, vysokokapacitných úložísk dát, detektorov žiarenia a iných zariadení. Vysokofrekvenčná elektrónová paramagnetická (VF-EPR) spektroskopia je vedecká disciplína skúmajúca, štrukturálne a magnetické vlastnosti týchto látok. Témou tejto práce je návrh nerezonančných držiakov pre VF-EPR spektrometer, určených pre rôzne typy vzoriek, najmä peliet z lisovaného prášku a nano-elektrických zariadení umiestnených na čipe. Výsledkom práce sú tri kalibrované prototypy držiakov, ktorých funkčnosť je otestovaná meraniami.

KLÍČOVÁ SLOVA

Vysokofrekvenčná elektrónová paramagnetická spektrometria, držiak vzorky, práškové spektrum, bolometer

ABSTRACT

Paramagnetic compounds and nano-electronic devices can find use in the development of quantum computing, high capacity data storages, irradiation detectors, and other devices. High-field electron paramagnetic (HF-EPR) spectroscopy is a scientific discipline for researching, structural, and magnetic properties of these materials. The theme of this thesis is the design of non-resonant sample holders for HF-EPR spectrometer, proposed for various types of samples, especially for powders pressed into pellets and nano-electronic devices placed on a chip. The result of this work is three calibrated prototypes of holders, which functionality is proved by measurements.

KEYWORDS

High-field electron paramagnetic resonance, sample holder, powder spectra, bolometer

BIBLIOGRAPHIC REFERENCE

LAGIŇ, Adam. *Design of non-resonant sample holders.* Brno, 2020. Available at: https://www.vutbr.cz/studenti/zav-prace/detail/124733. Bachelor thesis. Brno University of Technology, Faculty of Mechanical Engineering, Institute of Machine and Industrial Design. Thesis supervisor: Antonín Sojka.

ACKNOWLEDGMENT

The main acknowledgment belongs to Ing. Antonín Sojka for his supervision, submitted experiences, and active approach during the whole time. I would like to also thank to the leader of the MOTeS group in the CEITEC BUT Dr. Ing. Petr Neugebauer, who funded this project and enabled its realization, to consultant Ing. Aneta Zatočilová, Ph.D., and Dr. Ing. Vinicius Santana for their factual bits of advice and naturally to my nearest for their support during the whole study.

DECLARATION

I declare that the bachelor's thesis is my work under the supervision of Ing. Antonín Sojka and that all literature sources are listed in references and quoted completely and correctly.

…….

Author`s signature

CONTENTS

1 INTRODUCTION

Nanotechnology has a broad area of application such as in pharmacy, mechanical engineering, and electronics. One of these applications, such as storage devices and sensors, requires the proper characterization of paramagnetic molecules deposited on surfaces such as graphene or silicon. The characterization involves not only the proper detection and topography of formed nanostructures but also the control of their behavior as compared to bulk samples. Motivated by this demand the electron paramagnetic resonance (EPR) spectroscopy is an expanding scientific area.

EPR is a well and longtime known phenomenon. The first successful experiment with EPR spectroscopy was performed in 1944 by the Soviet physicist Yevgeny Zavoisky in Kazan, thanks to the rapid improvement of microwave technologies during the second world war. In 1957, when the importance of higher irradiation frequency was mentioned by George Feher to increase the sensitivity and resolution of signal detection, the development of EPR spectrometers working in high magnetic field and microwave frequency was challenging for many scientific groups around the world. Until this time, the X-Band frequency of radiation ($\approx$ 9.6 GHz) and magnetic field around 0.4 T was the most used. It was dependent on microwave and electromagnetic systems available at that time.

For performing an EPR experiment the placement of the sample in the right working conditions is important. For this purpose, cavities, resonators, or non-resonant sample holders are used. This thesis presents the design of non-resonant sample holders for high field electron paramagnetic resonance (HF-EPR) spectrometer for solving current requirements in this field. Designed sample holders deliver powder pellet samples or precise devices such as bolometers or semiconductors into high field electromagnet. In this work, the working environment of the area near the sample and universality of sample holders are taken into account to make the work with the spectrometer more efficient. The basics of the EPR spectroscopy technique and the construction of the HF-EPR spectrometer are described. Measurements confirm the functionality of the designed sample holders.

2 STATE OF ART

2.1 Electron Paramagnetic Resonance

In the following chapter, the essential theory needed for the understanding of electron paramagnetic resonance is described. The electron spin, Zeeman effect, and EPR spectra observation are described.

2.1.1 Electron spin

Electron paramagnetic resonance spectroscopy (EPR), also called electron spin resonance spectroscopy (ESR) is a precise technique for the description of paramagnetic samples, namely substances that have unpaired electrons. To explain EPR phenomena, we take elementary particles - electrons, which are characterized by an intrinsic angular momentum called spin. It can be defined as a vector with magnitude and direction. The magnitude of the electron spin angular momentum is quantified as [1]:

$$|\vec{S}| = \hbar\sqrt{s(s+1)} \tag{2.1}$$

where $s = 1/2$ is electron spin quantum number and there is convection to consider the angular momentum $\vec{S}$ and its components in $\hbar$ units (reduced Planck's constant $\hbar = h/2\pi$).

The electron spin is quantized and can be in two states, which we indicate as α and β. They are defined with components S_z along the axis z. These two states differ in the orientation but not in magnitude and according to quantum mechanics these S_z components assume values $1/2\ \hbar$ for α state and $-1/2\ \hbar$ for β state. Components in other directions of the x and y-axis are not necessary to be defined for our purpose. From these assumptions we can declare that α and β spins can exist anywhere on the surface of a cone:

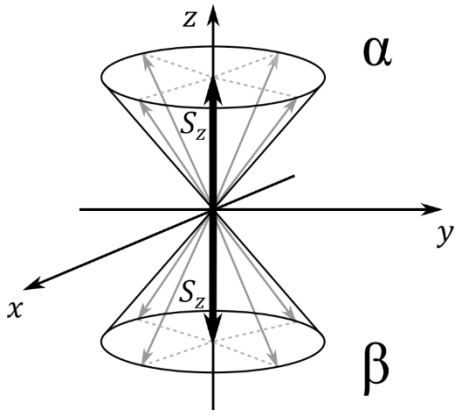

Fig. 2-1 Figure of electron spin angular momentum (grey arrows) and its S_z components (black arrows) [1].

2.1.2 Zeeman effect

Because of the charge of an electron, the angular motion of the particle generates a magnetic field. We can describe this phenomenon as a little bar magnet [2] with a magnetic moment $\vec{\mu}_e$ [3]:

$$\vec{\mu}_e = -g\mu_B\vec{S} \tag{2.2}$$

where $g = 2.002319$ [4] (for a free electron) is the Landé factor or so-called g-factor and $\mu_B = 9.274009 \cdot 10^{-24}\,\mathrm{J\,T^{-1}}$ [5] is the theoretical conversion constant called Bohr magneton. Due to the negative charge of the electron, the angular momentum $\vec{S}$ and magnetic the moment $\vec{\mu}_e$ have the same orientation but opposite direction.

When we place the electron near the external magnetic field $\vec{B}$, the energy of electron magnetic moment is given as:

$$E = -\vec{\mu}_e \cdot \vec{B} = g\mu_B\vec{S} \cdot \vec{B} \tag{2.3}$$

Due to interactions between the magnetic field $\vec{B}$ and magnetic moment $\vec{\mu}_e$, we can modify equation 2.3 to:

$$E = g\mu_B S_z B_0 \tag{2.4}$$

where B_0 is the intensity of the external magnetic field, $S_z = \pm 1/2$ is the z component of the spin. Thus, the electron can exist in the two energy levels (for α and β state) in the external magnetic field:

$$E_{\alpha,\beta} = \pm(1/2)g\mu_B B_0 \tag{2.5}$$

In case $B_0 = 0$, the energy is degenerated (the same for both states), but if $B_0 \neq 0$, the degeneracy is lifted, and we can observe the different energy for each state. The electron can switch from the lower energy level β to the higher energy level α by absorption of electromagnetic radiation with energy quantum equivalent to the energy difference of both states:

$$h\nu = \Delta E = |E_\alpha - E_\beta| = g\mu_B B_0 \tag{2.6}$$

where $h = 6.626068 \cdot 10^{-34}\,\mathrm{J\,s^{-1}}$ [6] is Planck's constant and ν is frequency of the radiation. In the described conditions, the absorption of electromagnetic radiation, usually in the microwave (MW) range, consists in the continuous-wave EPR experiment. The electron spin energy level separation is called the Zeeman effect (see Fig. 2-2). Thanks to this phenomenon, we can observe EPR spectra, convenient for the determination of the properties of paramagnetic materials.

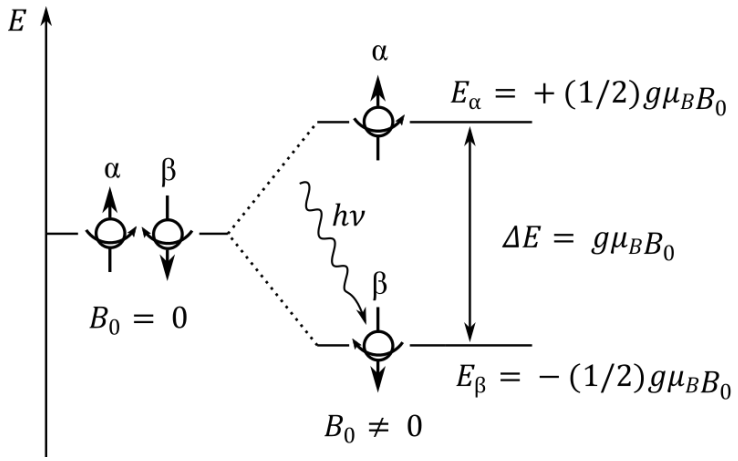

Fig. 2-2 Zeeman effect [2]: it describes the degeneration of electron spin at zero-field and split into two energy levels in the presence of a magnetic field. In case the correct magnetic field B_0 and frequency of microwave ν are matched, absorption of radiation can be measured.

2.1.3 The spin Hamiltonian

The Zeeman splitting of the electron is not the only information contained in the measured spectra. Samples contain several nuclei with spin and interacting electrons. These nuclei interact with unpaired electrons and cause additional energy level splitting. The energy of paramagnetic species in the ground state can be described by an effective spin Hamiltonian that includes all types of energy splitting [7], [8]:

$$\mathcal{H} = \mathcal{H}_{EZ} + \mathcal{H}_{HF} + \mathcal{H}_{ZF} + \mathcal{H}_{NQ} + \mathcal{H}_{EE} + \mathcal{H}_{NZ} + \mathcal{H}_{JT} \qquad (2.7)$$

where each component includes:

$\mathcal{H}_{EZ}$ – Electron Zeeman interaction (Zeeman effect – mentioned above), including spin-orbit interaction, caused by the orbital angular momentum of an electron.

$\mathcal{H}_{HF}$ – Hyperfine interaction, describing the interaction between electron and nuclei.

$\mathcal{H}_{ZF}$ – Zero-field interaction, explaining energy level states degeneration at the zero magnetic fields.

$\mathcal{H}_{NQ}$ – Nuclear quadrupole interaction, characterizing impact of layout of charge in the nucleus.

$\mathcal{H}_{EE}$ – Electron-electron interaction.

$\mathcal{H}_{NZ}$ – Nuclear Zeeman interaction, describing the Zeeman effect analogous for a nucleus, which changes its energy level according to magnetic field similarly as an electron.

$\mathcal{H}_{JT}$ – Jahn-Teller coupling interaction, characterizing splitting caused by electronic states affected by crystal lattice vibrations.

The description of energy level splittings caused by all interactions is convenient to determine the structural and magnetic properties of paramagnetic materials. Thus, we can observe the unique spectra and determine the Hamiltonian by simulations, which is like a fingerprint for each sample [9].

2.1.4 Frequency-domain and field-domain comparison

There are several ways of performing the EPR experiment. However, for our purposes, two methods will be described. The first method is consists of sweeping the frequency of the MW radiation with a constant magnetic field, which is very challenging because of the technical difficulties involved in producing a fluent and continuous change without loss of MW power through the wide frequency band [10]. This method is also called frequency-domain EPR spectrometry (see Fig. 2-3 a.)).

The second, more common, is by sweeping the magnetic field and irradiating the sample with a constant MW radiation frequency. When the correct magnetic field is reached, the absorption of the radiation can be measured [1]. This method is called field-domain EPR spectroscopy (see Fig. 2-3 b.)).

In the practical implementation of EPR spectrometers, the first derivative of the absorption signal is the most often measured signal. That is the outcome of the phase-sensitive detection [11] with a lock-in amplifier to reduce the signal-to-noise ratio. The modulation coil for this detection scheme is described in chapter 2.3.1.

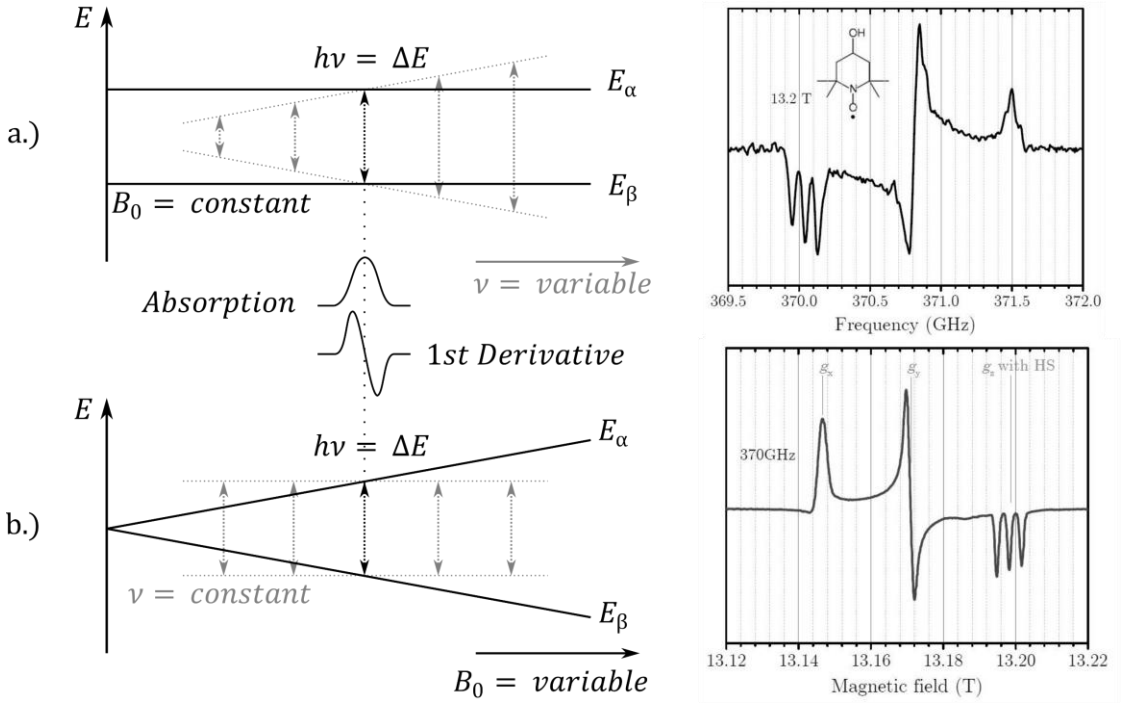

Fig. 2-3 EPR spectra observation [1]: a.) Frequency-domain and example of spectra; b.) Field-domain and example of spectra, spectra are measured on the TEMPO sample by Dr. Ing. Petr Neugebauer at the University of Stuttgart.

2.2 Reason for high magnetic fields in EPR spectroscopy

This section discusses the main advantages of HF-EPR spectrometers as the increased sensitivity due to Boltzmann distribution, and higher spectral resolution.

2.2.1 Boltzmann distribution

A typical sample for EPR spectroscopy contains thousands of molecules with unpaired electrons where the detected signal represents the absorption of the microwave by these electrons at a certain energy level. Therefore in a two-energy-level system, the ability of the sample to absorb microwave radiation depends on the ratio between the population of electrons in α and β energy levels, which is given by the Boltzmann distribution law [1]:

$$\frac{N_\alpha}{N_\beta} = e^{-h\nu/k_B T} \tag{2.8}$$

where $k_B = 1.38065(26) \cdot 10^{-23} JK^{-1}$ [12] is the Boltzmann constant, and T is the thermodynamic temperature of the sample. The ratio at room and cryogenic temperatures and at several frequencies are shown in Tab. 2-1:

Tab. 2-1 Ratios of electrons in α and β energy level for a low and high magnetic field.

Frequency band	**Frequency** (GHz)	**Magnetic field for *g*-factor=2** (T)	N_α/N_β **at T=293.15 K**	N_α/N_β **at T=1.8 K**
X-Band	≈ 10	0.357	998/1000	766/1000
Q-Band	≈ 40	1.427	993/1000	344/1000
W-Band	≈ 90	3.211	985/1000	91/1000
Y-Band	≈ 420	14.986	933/1000	14/100000

For $N_\alpha/N_\beta = 1$, the population among the different states is the same, and no absorption signal can be observed. As the ratio decreases, electrons start to occupy the lower energy level with higher probability. The lower the ratio, the stronger is the absorption and the more intense is the EPR signal. From Tab. 2-1, it can be observed that the best results are obtained for higher irradiation frequencies and lower temperatures, where the ratio is $N_\alpha/N_\beta \ll 1$.

2.2.2 EPR Spectra resolution increase

When the sample contains two or more species with different *g*-factors, it can be difficult to distinguish their signal in EPR spectra. The resolution is improved, when the magnetic field and frequency of irradiation is raised [9], as can be seen in the picture (Fig. 2-4):

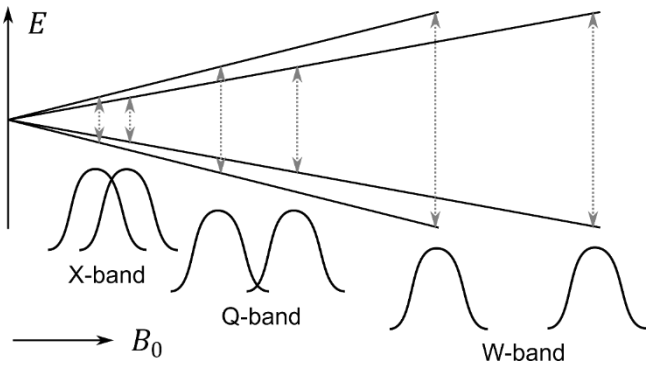

Fig. 2-4 Resolution increase in EPR absorption signal due to higher frequency (mag. field) [9].

It means that the signal from different species with different *g*-values in the sample can be recognized. Also, other EPR spectra features such as zero-field and hyperfine splitting can be detected only by experiments at higher frequencies and magnetic fields [13].

2.3 High-field EPR spectrometer

This chapter contains a brief discussion about the hardware of the high field EPR (HF-EPR) spectrometer at CEITEC BUT, necessary to understand its building and functionality. The spectrometer is working in continuous-wave mode, including frequency and field-domain, but also in the rapid frequency scan mode. It is available to perform measurements in a wide range of magnetic fields (up to 16 T), and frequencies (80 – 1100 GHz).

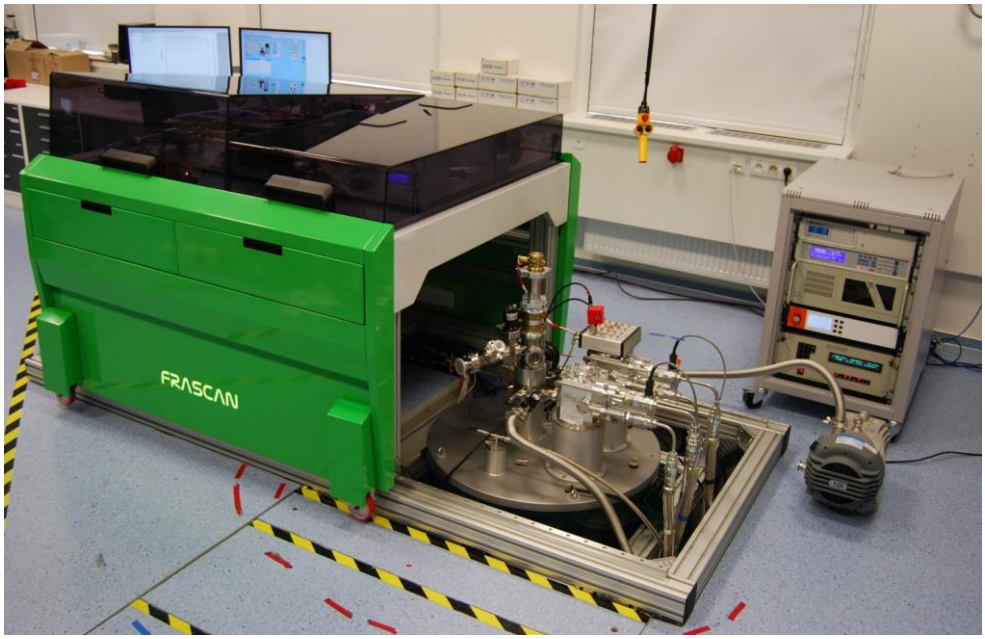

Fig. 2-5 HF-EPR spectrometer at CEITEC BUT (See detailed picture in attachment A6-1).

Most of the HF-EPR spectrometers work in the field-domain, with the sample continuously irradiated by MW. Therefore, every optical component is optimized for one frequency. In our case, we can sweep with the magnetic field and frequency, which requires a frequency-independent optical component for manipulation of the MW beam. For this reason, quasi-optics is used. The initial MW beam is radiated from the source and is split into reference and irradiation arm. The irradiation arm propagates to the sample situated in the center of the magnet and is reflected by a mirror under the sample back to the detector via the "quasi-optical circulator" and system of mirrors [14]. The detection of the signal using one MW source is called homodyne signal detection. The whole setup can be seen in the simplified scheme (Fig. 2-6):

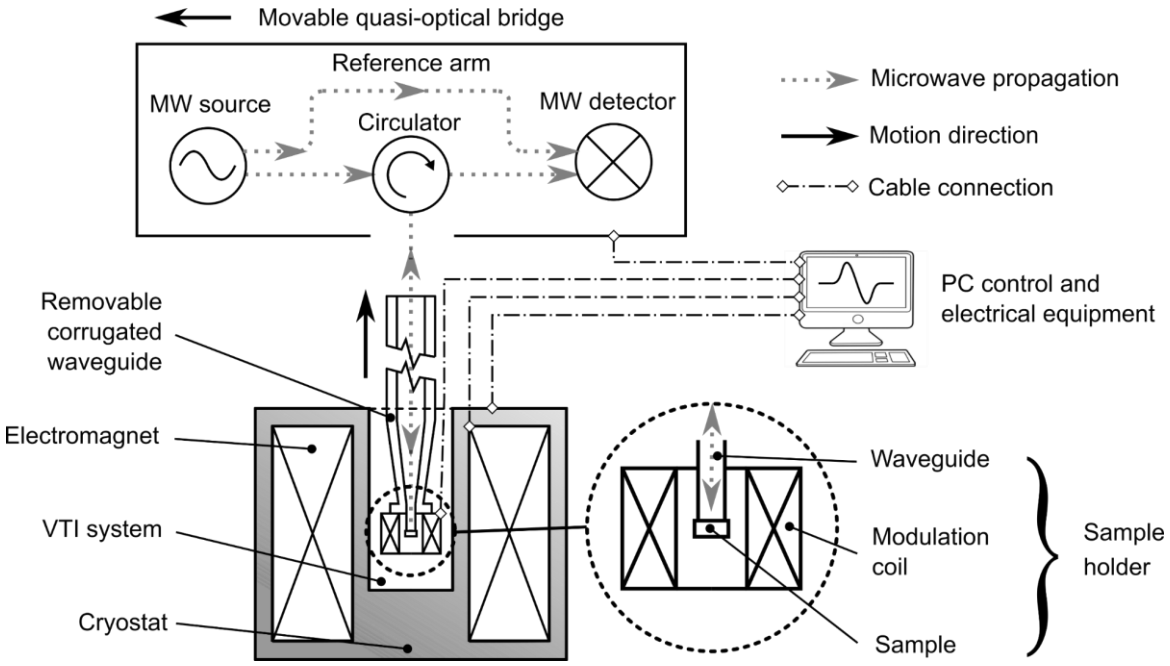

Fig. 2-6 Scheme of HF-EPR spectrometer in homodyne detection mode.

2.3.1 Microwave source, detector, and modulation coil

MW sources: Most of the MW sources usable for EPR spectroscopy can be assorted into two main groups: vacuum-tube oscillators and solid-state oscillators. Nowadays due to costs, reliability, and size, solid-state microwave sources are preferred [15].

MW detectors: Concerning the detection, EPR spectrometers are using bolometers or solid-state based Shottky diodes [16]. Bolometers are precise devices that detect electromagnetic radiation by converting it to heat. A small heat change gives rise to a large resistance change, which can be measured. The ability to amplify the resistance change makes the bolometer an extremely sensitive radiation detector, especially when it is working in low temperatures [17].

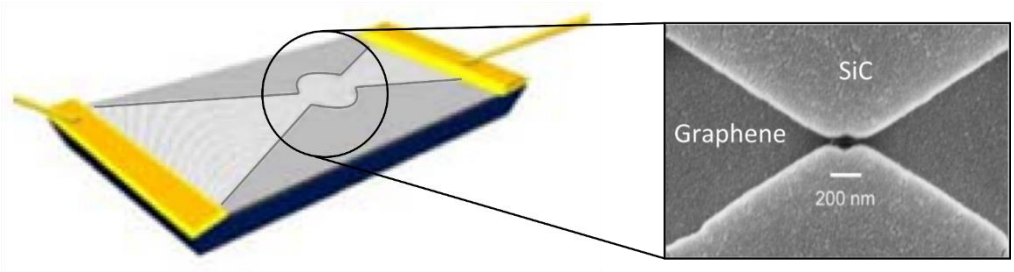

Fig. 2-7 Quantum dot graphene bolometer. Taken from [18] and adjusted.

Bolometers operate in multi-frequency mode, but because of slow response, they are typically used for spectrometer working in the field-domain. Shottky diodes as detectors are more popular for Pulse EPR and frequency-domain EPR for their accuracy and fast response [19].

Modulation coil: The modulation coil is employed to enhance the sensitivity of the EPR spectrometer by producing an additional alternating magnetic field with a small amplitude along with the magnetic field of the main EPR magnet. As a result, the absorbed signal is modulated by the frequency of the modulation coil. Then, the modulated signal from the detector is processed by a lock-in amplifier and matched with the input signal of the modulation coil. The product of this signal processing is the first derivative of the absorption signal. Tunable modulation frequency and amplitude allow to reduce noise and enhance the signal. Wrong modulation settings can ruin the measurements with an artifact, excessive noise, or decrease of spectra resolution [11].

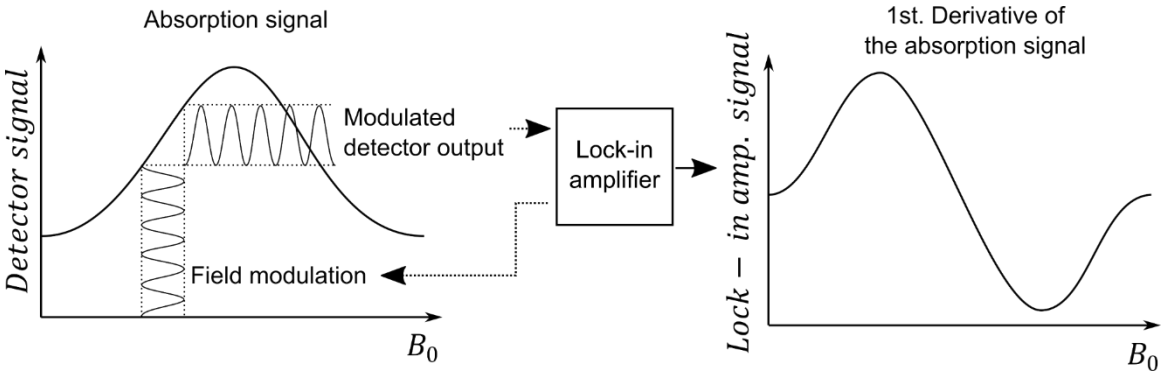

Fig. 2-8 Modulation of the magnetic field, and its effect on EPR signal [2]: The modulation of the magnetic field causes enhance of EPR spectra and its first derivation.

2.3.2 Microwave propagation

The EPR spectrometer at CEITEC BUT uses a quasi-optical bridge for the MW propagation. The main advantage of the quasi-optics is its ability to work in a wide range of frequencies and low power losses in comparison with classic waveguides [15]. For separation of the signal carrying MW and non-affected MW, the “quasi-optical circulator” is used. It is a system of polarizers and Faraday rotator [20] using the fact that the MW affected and non-affected by the sample have different polarization [9]. The quasi-optical bridge is out of the scope of this work, so its full description can be found in [14].

A corrugated waveguide propagates the microwave between the quasi-optical bridge and the sample placed in the center of the magnet [21]. Corrugation helps to propagate MW in a closed space and significantly reduces the loss in MW power [20]. A corrugated taper on the end of the waveguide focuses the beam on the sample/mirror within the sample holder. The assembly of the waveguide and sample holder covered with a shielding tube creates the probe (see attachment A6-2), which has to be pulled out from the cryostat when the sample should be replaced. The removal of the probe is allowed by the movable quasi-optical table (see attachment A6-1).

2.3.3 Cryostat and superconducting electromagnet

The superconductive electromagnet creates a homogenous magnetic field with a precisely defined direction. The magnetic field intensity is swept thanks to the change of an electric current running in the superconducting coils. The magnetic field can reach up to 16 T. The coil has to be cooled down below 10 K to guarantee the superconductivity state. The low-temperature environment is provided by a cryostat in which the electromagnet is situated. The cryostat is also equipped with a variable temperature insert (VTI) system, which can change the temperature of the environment in the center of the electromagnet and therefore provide different conditions for characterizations of a sample. The usual temperature range is from 1.6 K to 325 K [22]. The VTI system works with a flow of helium gas as a cooling medium that has a high specific heat capacity [23] (in comparison with metals at low temperatures).

2.3.4 Sample holder

In EPR spectroscopy, we are interested in the interaction of the magnetic component of MW with electrons in the sample. Therefore, in the majority of EPR spectrometers, the sample is placed inside a sample holder called a resonator, also called a sample cavity. The resonator has a calculated dimension to create standing waves with a maximum of the magnetic component of MW in a small area around the sample. This approach helps to improve the signal-to-noise ratio [11].

The typical resonator is a single-mode cavity, which is simply a metal box in a rectangular or circular shape [11] (see Fig. 2-9). The dimensions of the cavity are chosen according to the exact microwave frequency, which makes it impossible to use a resonator for frequency-domain experiment.

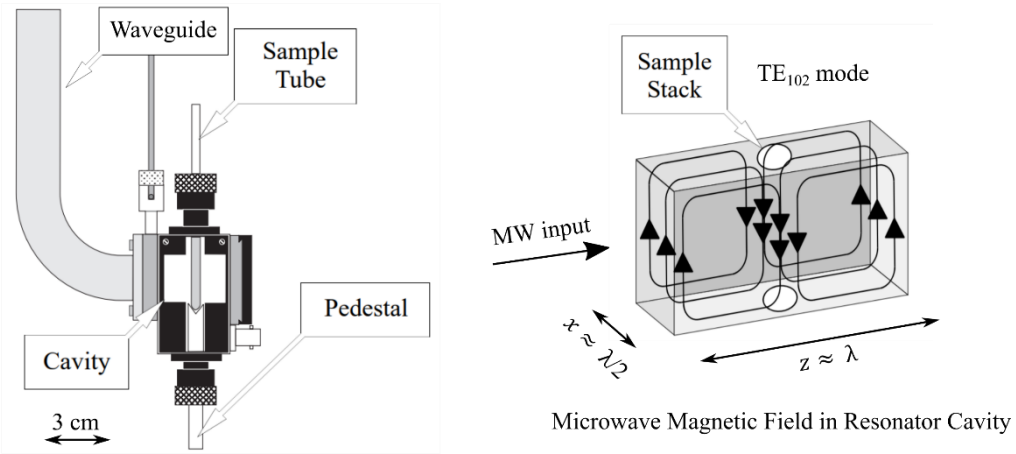

Fig. 2-9 Scheme of a Bruker X-band sample holder (resonator) and the most used rectangular TE_{102} mode cavity. Taken from [24], [11] and adjusted.

The single-mode cavities are commonly commercially available. However, the increasing radiation frequency requires smaller dimensions of the cavity and thus space for sample, which means, it is not practical for HF-EPR spectroscopy [16]. At the frequency of 420 GHz, the cavity is so small, that the handling with the sample would be very difficult, as can be seen in Tab. 2-2:

Tab. 2-2 Examples of rectangular TE_{102} mode cavity dimensions for low and high frequencies.

Frequency band	**Frequency** (GHz)	**x-dimension** (mm)	**z-dimension** (mm)
X-Band	≈ 10	≈ 15	≈ 30
Q-Band	≈ 40	≈ 3.75	≈ 7.5
W-Band	≈ 90	≈ 1.65	≈ 3.3
Y-Band	≈ 420	≈ 0.35	≈ 0.7

Such a problem of dimensions in higher frequencies can be solved with a Fabry-Pérot resonator (see Fig. 2-10). It contains two mirrors specially designed for a particular microwave frequency [25]. The advantage is the increased area for a sample volume that is much larger than in the single-mode cavity [15].

Another solution to solve the problem is the use of non-resonant cavities (see Fig. 2-10). According to Eq. 2-8, when low temperatures and high frequencies are used for an experiment, the sensitivity even without resonance cavity is satisfying for most experiments [9]. The main advantage of the non-resonant sample cavity is that it can be used in a wide range of frequencies.

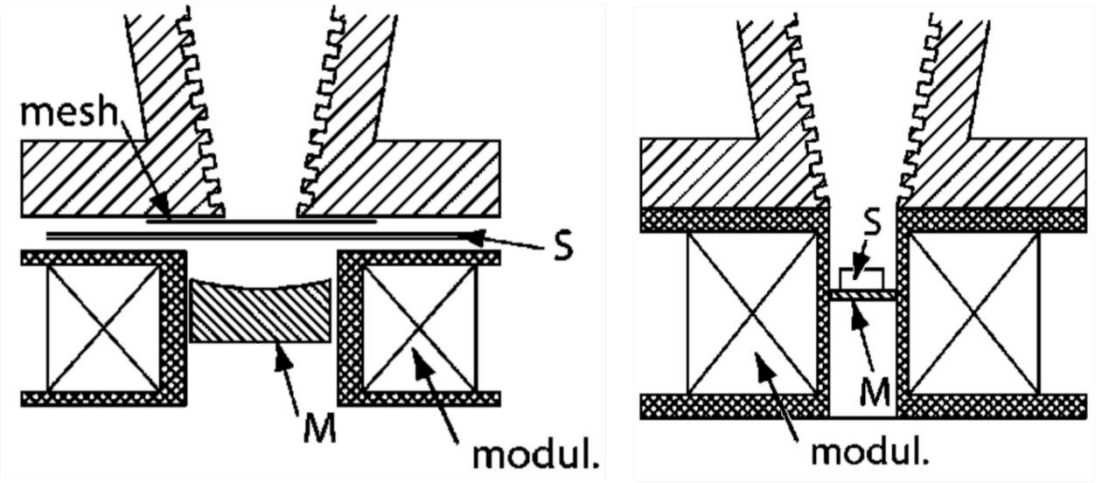

Fig. 2-10 Left: scheme of half-symmetric Fabry-Pérot resonator. Right: scheme of a non-resonant sample cavity. (M – mirror, modul – modulation coil, S – sample, mesh – semi transient mirror). Taken from [26] and adjusted.

Typical samples for HF-EPR spectroscopy have the form of a pressed powder, called a pellet. However, the HF-EPR can also be used for liquid and crystal samples. In our setup, electric properties by transport measurements are available too. To be able to study all those systems in frequency-domain EPR, non-resonant sample holders are necessary. Each non-resonant sample holder has to be equipped by a modulation coil to enhance the signal-to-noise ratio, waveguide to lead MW to the sample, and mirror to reflect the MW beam to the detector.

3 PROBLEM ANALYSIS AND AIM OF THE THESIS

3.1 Aim of the thesis

This thesis aims to design and construct three non-resonant sample holders for HF-EPR spectroscopy:

- Sample holder for one pressed powder pellet,
- Sample holder for a chip expander, which is designed to perform transport measurements,
- Carousel sample holder, a unique holder able to deliver several pressed powder pellets at once to the spectrometer, decreasing the time consumed by the sample changing process.

Each sample holder has to fulfill the conditions described in section 3.2. Since the HF-EPR spectrometer is used for different scientific purposes and thus for different sample holders, an important aim of the thesis is also to design a universal loading mechanism for all types of sample holders, ensuring fast loading and easy electrical connection.

3.2 Conditions and working environment

In the following sections, sample conditions for the EPR experiment and the associated problems with the construction of sample holders are summarized.

3.2.1 Avoiding magnetic and conducting material

During the EPR experiment, the sample is placed into the center of a strong homogenous magnetic field, which can reach up to 16 T. The measurement is very sensitive to any small displacement of the sample from the center of the magnetic field. Therefore, it is necessary to avoid magnetic materials for the sample holder design because of possible movements during the sweep of the magnetic field.

Each sample holder has to be equipped with a modulation coil to create a homogenous alternating magnetic field with sufficient amplitude in sample space to enhance the EPR signal. The modulation coils have a typical intensity of 0.1 – 1 mT and frequency from 1 kHz up to 100 kHz [15]. However, the enhancement of the EPR signal can be decreased by induced eddy current in a conductive material by the rapid change of intensity of the magnetic field [27]. Moreover, eddy currents can cause warming of the metallic materials and thus sample itself.

3.2.2 Low temperatures

EPR measurements are mostly performed with a sample placed into cryogenics temperatures, which enhance the EPR signal (Eq. 2-8). Thanks to the VTI system, the measurement can be performed in temperatures from 1.6 K to 325 K. To decrease the cooling time of the sample, it is necessary to design a light assembly. Moreover, big caution has to be taken to the material selection and their different temperature dilatation for movable components to keep their ability to move in low temperatures.

3.2.3 Dimensions

The size of the sample holder is limited by the bore of the airlock, which is a mechanism to enable to load a sample holder into the VTI without contamination of the helium atmosphere inside (see attachments A6-1 and A6-2). The maximum diameter which can be reached is 42 mm. The location from the end of the waveguide can be arbitrary, but the same for each sample holder.

3.2.4 Wiring

Precise nano-electronic devices, as mentioned bolometers (see chapter 2.3.1) are usually manufactured on Si wafer and placed on a chip expander (see Fig. 3-1) which helps to contact them with external scientific instruments. Therefore, the universal loading mechanism and the sample holder for carries chip has to be equipped with enough contact to be able to perform transport measurement.

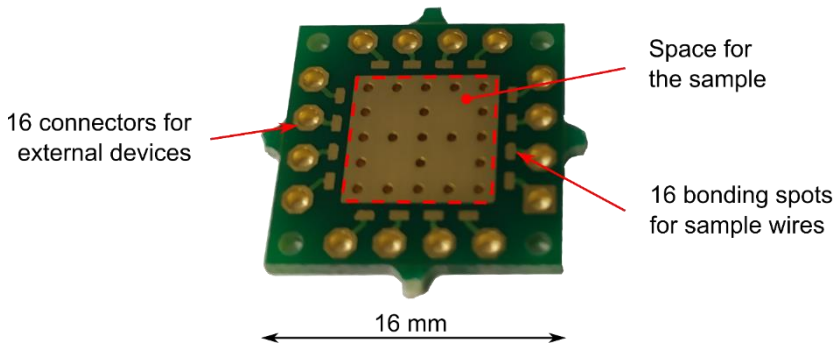

Fig. 3-1 Chip expander: it contains 16 golden plated bonding spots for sample connection and 16 connectors for external devices.

4 CONCEPTUAL SOLUTION

In this chapter, the technical concepts involved in the construction of the sample holder are discussed. At first, a solution of universal loading flange is presented. Then, the design concepts for different proposed sample holders are presented.

4.1 Sample holder attachment

The requirement for user-friendly handling and fast change of sample holders can be provided by the universal flange and locking mechanism. The sample holder would be attached by the universal flange mounted to the end of the corrugated waveguide. This flange would contain all required prepared connectors and cables. Such configuration avoids a mistake in the wiring, connection of sensors and other devices situated in the sample holders.

4.1.1 Attachment by screws

The first variant counts with screw fixation (see Fig. 4-1). The advantage is simple technological production, low production accuracy requirement, and low costs. On the other hand, the connection of the sample holder to the flange requires the usage of additional tools. Screws also have limited durability due to attaching/detaching cycles of the sample holder.

4.1.2 Bayonet mechanism

The second design considers the usage of a well-known bayonet mechanism. The functionality is warranted by the rotary collar with grooves and studs placed on the body of the sample holder (see Fig. 4-1). The advantages are that the additional tools are not needed, and the preparation of the probe can be performed in a few seconds. The whole mechanism is durable against repeating usage. However, the production accuracy and cost requirements are higher.

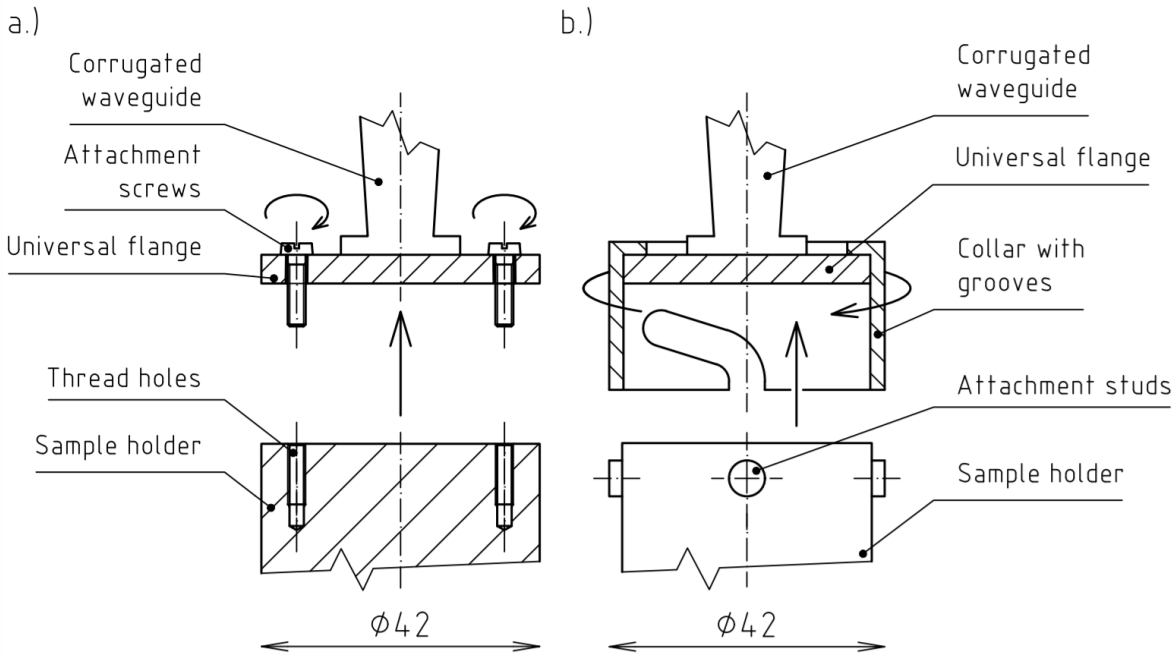

Fig. 4-1 Sample holder mount concepts: a.) Attachment by screws; b.) Bayonet mechanism.

4.2 Sample holders

All sample holders should work on a similar principle, to be user-friendly. Therefore, the concepts of the sample holders can be divided into two main groups by method of the sample loading. Each sample holder has to be equipped with the modulation coil, the temperature sensor, and a heater, which can provide fine sample temperature adjustment at low temperatures.

4.2.1 Bottom sample loading

The concept uses the functional part, which is screwed into the body from the bottom side (see Fig. 4-2). It guarantees the exact position of the sample in the middle of the modulation coil. The upper connector can be equipped with pins for connection of temperature sensor, heater, and chip expander devices. Thus, the bottom sample loading solution can be exploited for pellet sample holder, chip sample holder, or crystal rotator sample holder which is not part of this thesis.

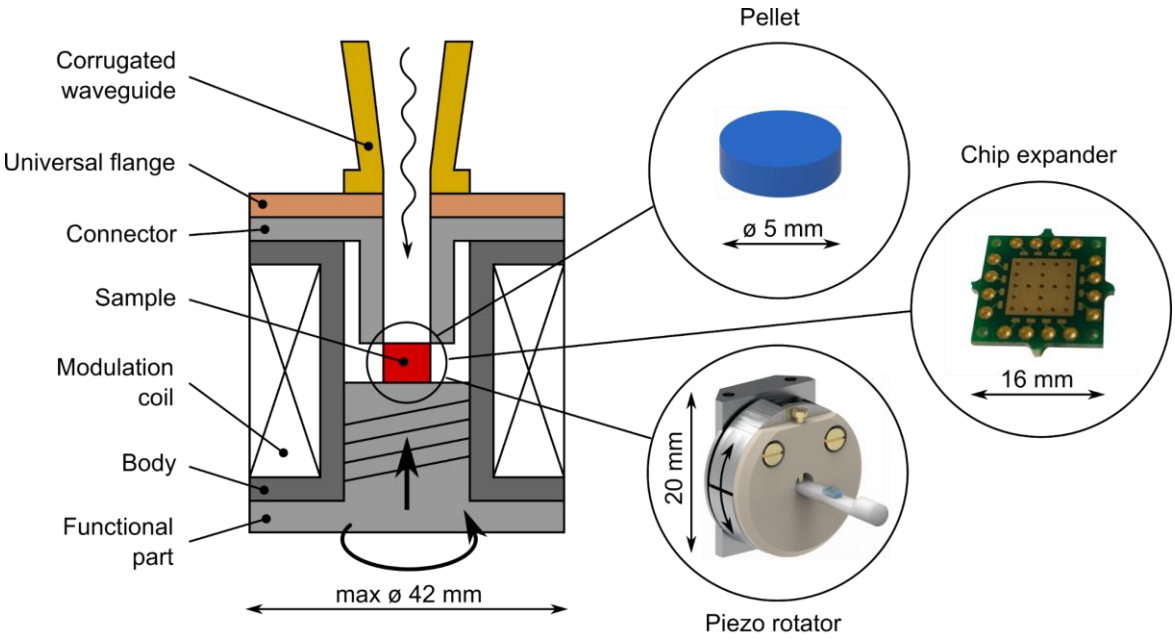

Fig. 4-2 Concept of the bottom loading system convenient for pellet sample, chip expander sample, piezo rotator for a single-crystal sample.

4.2.2 Side sample loading

The solution is based on the Helmholtz coil [28], which contains two separate coils with the same diameter and identical symmetry axis position to create the homogenous magnetic field between them. This fact allows us to create the space for side sample loading into the center of the modulation coil. This concept is convenient to be applied for a carousel sample holder, which can carry several pellets in one loading. The samples will be placed in a rotary platform - pallet. By rotating this platform, the chosen sample can be delivered under the waveguide and thus to the center of the modulation coil.

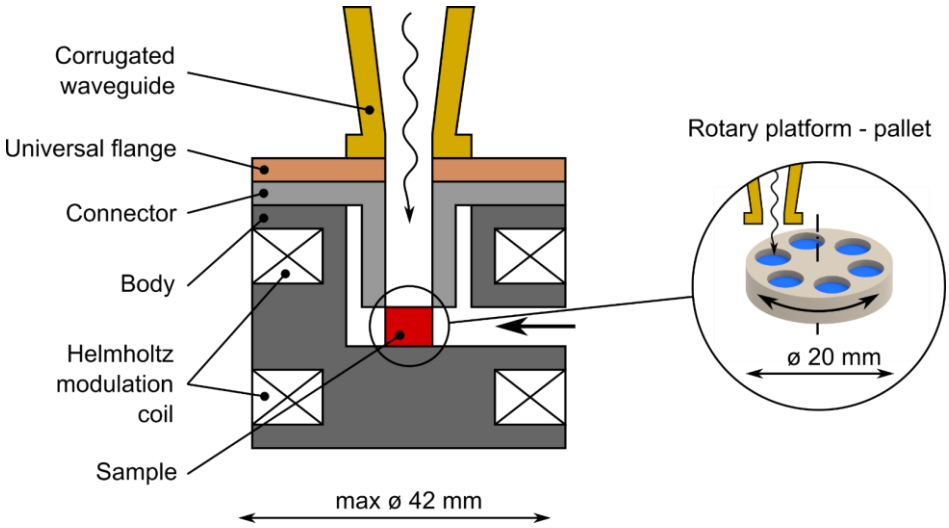

Fig. 4-3 Side sample loading convenient for a rotary platform - pallet filled with several sample pellets.

5 FINAL DESIGN

In this chapter, the final design of the sample holders is presented. All construction solutions are solved complexly and have common constructional signs to improve user-friendly handling.

5.1 Sample holder attachment

In this section, the universal sample holder bayonet mechanism with a wiring connection is described. The system needs to be equipped with 24 electrical connections to fulfill all requirements of each sample holder.

5.1.1 Loading mechanism

The construction uses the concept of the bayonet mechanism. Four grooves provide the fixation of the sample holder on the collar. The correct position of the attachment is warranted by one wider groove, which fits only in one specific thicker stud placed in the sample holders. A small dot marks the position of the wider grove and stud (see attachment A6-3). To make the handling simpler, the motion of the collar is limited by two stops screws adequately placed on the top of the collar, which allows motion in angle 40° only (see Fig. 5-1).

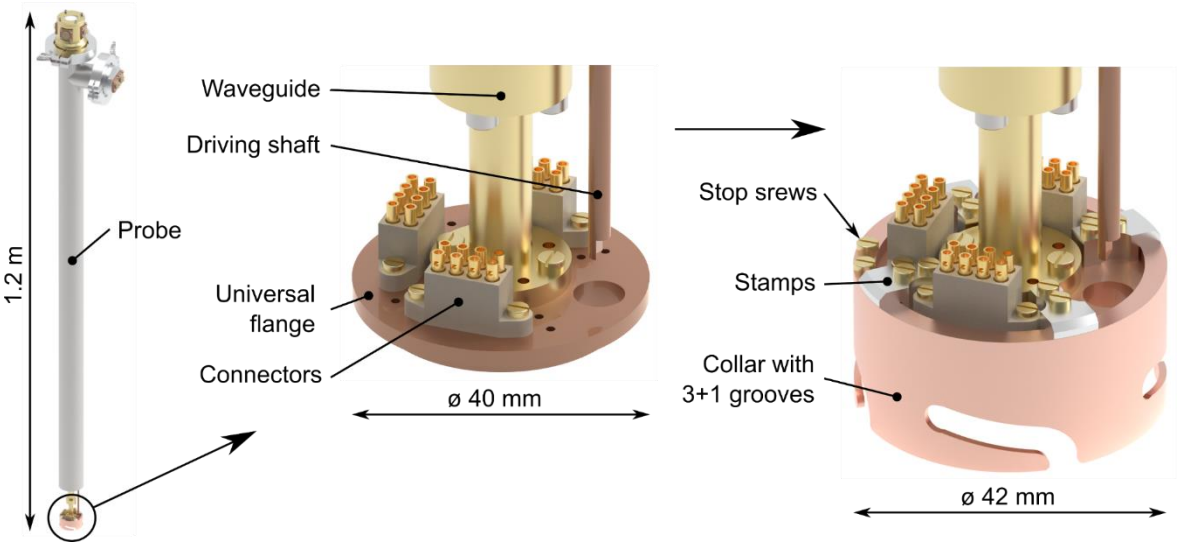

Fig. 5-1 Left: Probe with a detailed view on the design of the universal flange. Middle: Flange details. Right: Flange using bayonet mechanism to attach sample holders.

5.1.2 Wiring

Copper is commonly used material as a conductor, thanks to low electrical resistivity (see Tab. 5-1). In cryogenics applications, there arises a problem with the variability of resistance caused by various temperatures along the conductor (operation temperature is 1.6 - 300 K), which can cause inaccuracies in the measurement of devices placed in the VTI system. For devices such as modulation coil and heater, where the electric resistance is not measured, copper as a conductor is used.

The temperature sensor, where the temperature is measured as a function of resistance, is connected using the four-point-method [29]. In this configuration, only the resistance of the temperature sensor with its wiring inside of the sample holder is measured. Therefore, it allows the usage of copper wiring for the temperature sensor connection.

For devices that cannot be measured by the four-point technique, another conductor material has to be used to prevent the thermal variability of resistivity. It can be solved with materials with a lower thermal coefficient of resistivity (see Tab. 5-1). Because of relatively small electrical resistivity, the phosphor bronze was chosen as a universal cable material. The resistivity thermal coefficient is adequately low compared to copper, and electrical resistivity is also relatively low in comparison to other materials.

Tab. 5-1 Table of material electrical properties commonly used in cryogenics temperatures [30].

Material	**Chemical composition**	**Electrical resistivity at 293.15K** ($\mu\Omega \cdot cm$)	**Thermal coefficient of resistivity** (K^{-1})	**Reference**
Copper	Cu 100%	1.7	0.0039	[31]
Phosphor bronze	Cu 94 %, Sn 6%, P 0.01 – 0.3%	11 - 16	0.0007	[31]
Nichrome	Ni 80%, Cr 20%	108	0.00005	[31]
Constantan	Ni 45%, Cu 55%	52	0.00002	[31]
Manganin	Cu 86%, Mn 12%, Ni 2%	43 - 48	0.00001	[31]

5.1.3 Connectors

The universal flange has 3 removable connectors with 8 pins each (see Fig. 5-1). It means up to 24 wires can be used for the connection of devices. The number of pins was chosen according to measurement requirements and space on the flange.

Tab. 5-2 Table of the count of pins for selected devices and material of wires.

Device	Number of pins	Wire material
Modulation coil	2	Copper
Temperature sensor	2	Copper
Heater	2	Copper
Reserve pins	2	According to the connected device
Chip expander or another device	16	Phosphor bronze

Polyether ether ketone (PEEK™) as material for the connectors is selected, thanks to its low water absorption (≈ 0.3% of dry material weight) [32], which guarantees high durability to repeated cooling cycles. It is also convenient because it reduces the risk of contamination of the helium atmosphere in the VTI system with water. It has high dielectric strength (≈ 20 kV/mm) [33], which allows using this material as an insulator. The manufacturing quality of this material is very satisfying and suitable for small shape complex parts.

For connectors, Lewvac pins are used [34]. They are convenient to be used in an ultra-high vacuum environment. Their copper body warrants good conductivity, and the gold-plated surface reduces oxidation and reduces transient resistance. Lewvac pins are also supplied with special tongs that press the top of the connector and attach the wire without the necessity of the use of a solder [35].

The connection scheme for the universal flange connection is shown in the attachments (see attachment A1).

5.2 Pellet sample holder

The purpose of the pellet sample holder is to deliver one sample into the center of the magnet and perform the EPR measurement on it. The whole design can be divided into three main parts: connector, body, and functional part. Each part separately will be discussed.

5.2.1 Body

The body serves as a holder for the modulation coil (see Fig. 5-2). The modulation coil is made from copper wire insulated with a thin layer of Kapton®. The conductor is wounded on the body precisely, and each layer is fixed with glue.

The body also contains four studs, made from aluminum to attach the sample holder to the universal flange by the bayonet mechanism. Holes were drilled to the body to help the delivery of the cooling gas to the sample. The body has not any additional particular functionality. Because electrical insulation is required, the polyurethane (PU – Tufset) as a material was chosen due to its low price. This polymer also has very low water absorbance (≈ 0.1% of dry material weight) [36].

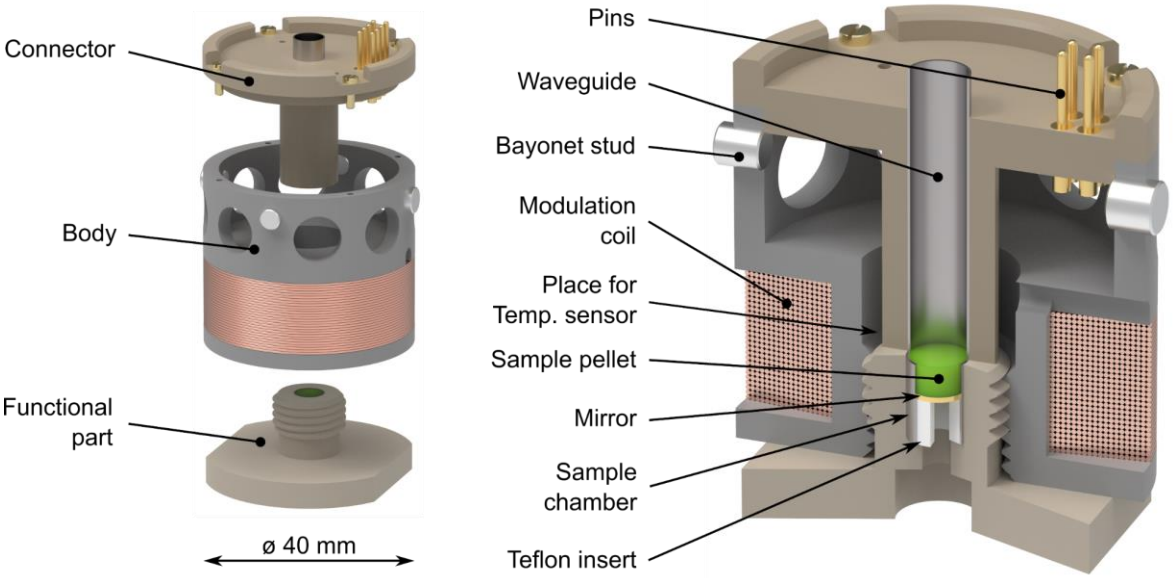

Fig. 5-2 Design of the pellet sample holder – disassembled into the main parts (on the left) and sectional view containing annotations of all parts (on the right).

5.2.2 Connector

The upper part (see Fig. 5-2) contains a connection for modulation coil and temperature sensor (see attachment A2). The accurate position of the connector to studs placed on the body is guaranteed with four screws. The waveguide for coupling MW from corrugated waveguide to the sample and back is pressed into the central hole.

The temperature sensor has to be placed as near as possible to the sample. It means, it is glued with thermally conductive epoxy on the edge of the waveguide. The heater is not required but can be situated on the body around the waveguide as near as possible to the sample.

The material used for the connector is PEEK ™ due to its properties mentioned above (see chapter 5.1.3).

5.2.3 Functional part

This part carries the sample and is screwed inside of the body. The sample is embedded in the small chamber with a mirror bounded to the waveguide, which reduces loss in microwave power. The position of the mirror can be adjusted by a Teflon® insert (see Fig. 5-2). The sample pellet is fixed with Teflon® tape, which has no EPR signal. The sample can be easily removed with a needle or any thin tool by pushing from the bottom.

5.3 Chip sample holder

In the next sections, the construction of the chip sample holder is described. The purpose of this holder is to carry the chip expander with electronic devices to perform transport measuring in EPR.

5.3.1 Body and connector

To help users to understand the functionality and usage, the chip sample holder comes out from the same concept as the pellet sample holder (see chapter 5.2.1). It means the body, similar to the pellet sample holder, carries the modulation coil. The connector contains all necessary pins for connection with the flange and functional part (see attachment A3). The main advantage is that all connectors are already prepared before sample loading. The connector is attached to the body via two screws and cylindrical pins (see Fig. 5-3).

5.3.2 Sample placement

The chip expander is a small circuit board with 16 golden plated holes (see Fig. 3-1). The sample is carried within the holder by the chip expander, which has to be connected with measuring devices. The measured device, prepared by lithography on a silicon surface, is glued to the center of the chip and then soldered to connection spots linked with gold plated holes.

The chip expander is placed on the rotary base of the functional part (see Fig. 5-3). A slight interference fit between pins and golden plated holes guarantees a reliable connection. The heat sink placed under the chip expander deceives the heat produced by dissipated radiation energy. This is very important for the measurement of bolometers, which are sensitive to any temperature change. The heat sink has to be non-conductive to prevent eddy currents produced by the modulated magnetic field. Sapphire is the chosen material for its good thermal conductivity at low temperatures and as considering non-conductive materials [37]. Thanks to the gap between the base and the sapphire block, a good cooling medium flow is provided.

The temperature sensor and the heater are situated and glued on the bottom surface of the sapphire board, which allows fine temperature adjustment of the sample.

The functional part after chip insertion is screwed into the body. Three position-studs warrant the correct position of the base connectors to upper part connectors on the base and guide grooves in the body. Their placement is selected so that there cannot arise the mistake in connection. The rotary base allows transferring rotary motion of the screw to linear motion of the base with connectors. These features make the sample holder more user-friendly.

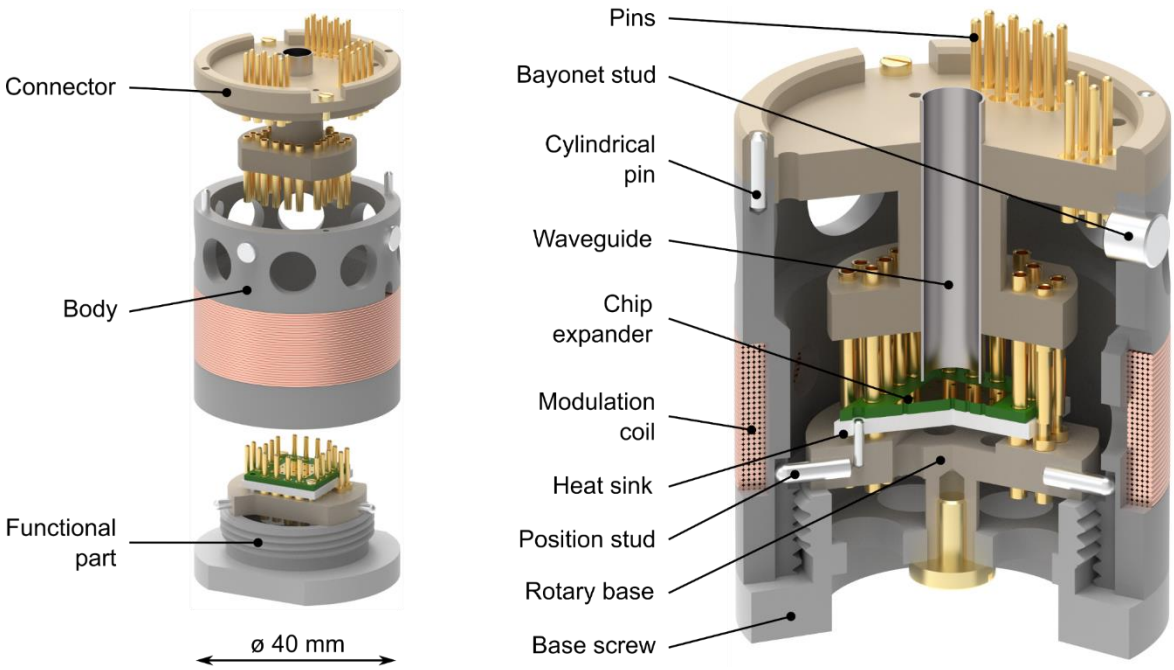

Fig. 5-3 Design of chip sample holder – disassembled into the main parts (on the left) and sectional view containing annotations of all parts (on the right).

5.4 Carousel sample holder

The carousel sample holder is designed to carry six samples at once. It helps to reduce the time of cooling and probe preparation. Construction and functionality are described in the next sections.

5.4.1 Body and connector

The body and connector have a similar purpose as described above for the other sample holders. However, the modulation is provided by two Helmholtz coils. One of them is placed on the connector and the other is under the sample platform. The Helmholtz coils provide a large area for the sample and allow a lateral loading of the samples (see Fig. 5-4). The functionality of the body is guaranteed by tolerances calculation (see attachment A5). The connection is described in attachments (see attachment A4).

5.4.2 Sample placement

Samples are evenly placed on the removable sample platform – pallet (see Fig. 5-4). Each sample chamber is equipped with two rings serving as fixation of the sample. The sample platform is fixed with a lock printed on a 3D printer from PETG filament. The mirror reflecting the radiation is placed in the disc carrying the second modulation coil. It allows using the sample holder for quantitative measurement because all the components involved in measurement (modulation, waveguide, mirror) will be the same except for the sample itself. This will allow us to quantify the EPR signal intensity of each sample, proportional to the number of paramagnetic molecules in a compound.

The temperature sensor is placed inside of the body to measure the temperature of the environment inside of the sample holder. Placement near to the sample is not possible, due to the rotary motion of the sample platform - pallet.

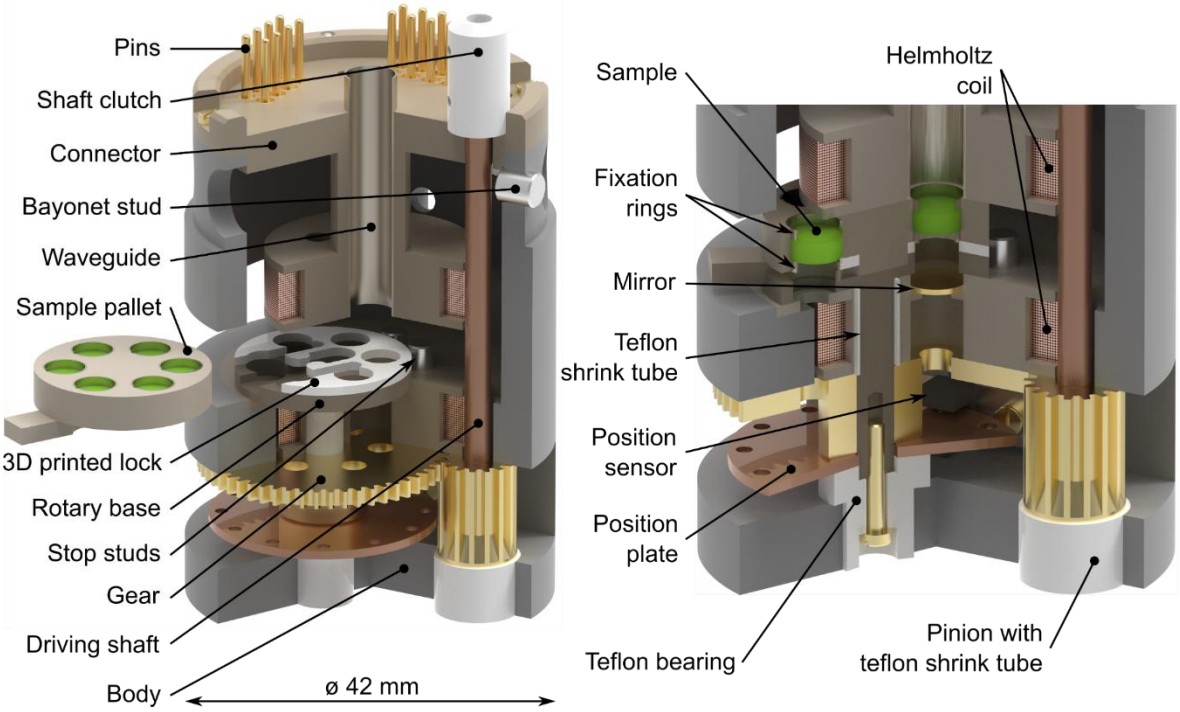

Fig. 5-4 Design of carousel sample holder – sectional views containing annotations of all parts, the whole assembly (on the left), and the detailed view to the rotary system (on the right).

5.4.3 Sample positioning

The samples (pellets) are placed on the rotary platform (sample pallet) situated out of the waveguide axis (see Fig. 5-4). It allows changing the sample with rotary motion. Torque is provided by a gear at the bottom of the sample holder. The gear conversion is chosen according to the axis distance of gears.

The ability of motion is guaranteed by Teflon® plain bearings or by separation of each part with Teflon® shrink tubes. This material was chosen due to its high thermal expansion coefficient, which is at least two times higher than PEEK ™ or Tufset. It causes, the fine fittings between movable parts will be preserved at low temperatures.

Tab. 5-3 Table of material thermal coefficient of expansion.

Material	Thermal coefficient of expansion at 273.15 K (10^{-6} /°C)	Reference
PEEK ™	≈ 48	[38]
PU - Tufset	≈ 80	[39]
PTFE - Teflon®	200	[40]

The correct position of the sample is checked by a plate with holes and a photo microsensor Omron EE-SX1230 [41]. The plate is aligned with the sample platform. When the light goes through the hole in the plate, the photosensor approves the right position. The whole system is driven by a gearbox situated on the top of the probe. The gearbox and piezoelectric motor are designed inside of the probe tube and connected through vacuum sealing connectors (see Fig. 5-5). Piezomotor is chosen, due to its ability to work in a low vacuum and its small step of rotary motion, which allows fine positioning [42].

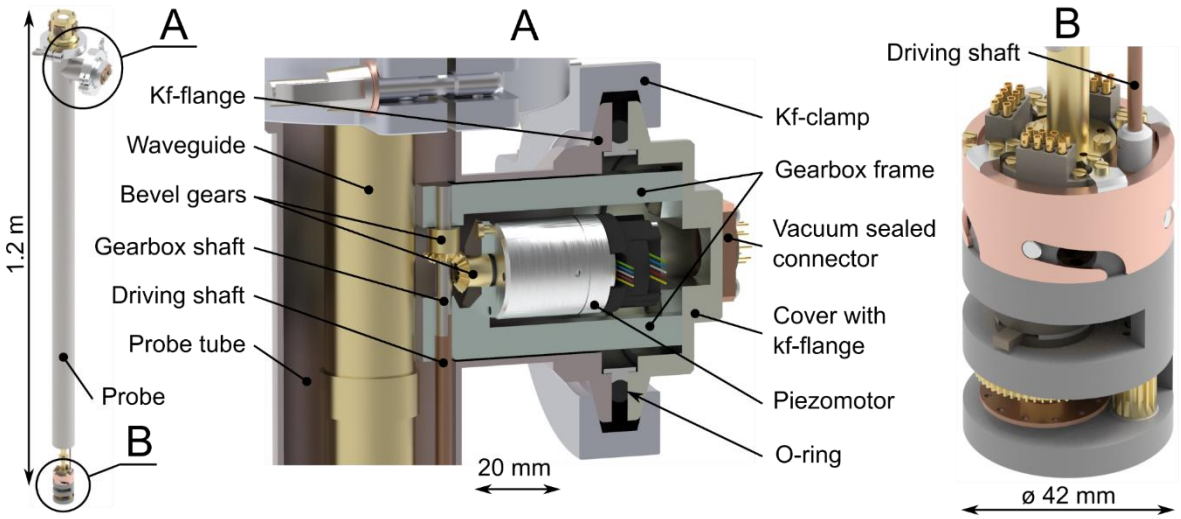

Fig. 5-5 Design of the probe for carousel sample holder: A – gearbox – sectional view with all parts, B – carousel sample holder mount.

6 DISCUSSION

6.1 Modulation coil calibration

As mentioned before, the modulation coil can significantly improve the signal-to-noise ratio. For proper measurement, it is important to know the exact amplitude and frequency of the modulated magnetic field. It can be warranted by calibration when the amplitude of the magnetic field is measured as a function of the amplitude of the alternating current flowing in the coil.

The first way to perform a calibration was by using a Hall effect sensor. This method proved not very reliable because the sensor's sensitivity considerably depends on its position in the magnetic field and its orientation with respect to the field lines. This fact makes the experiment much more difficult due to the size of the sample chamber, where the Hall effect sensor should be precisely situated.

The second more reliable method is by the measurement of a LiPc (Lithium Phthalocyanine) sample, which has in the structure one free electron. The sample itself has a very narrow EPR signal, which is convenient for modulation coil calibration. The idea is to perform a frequency-domain experiment (see chapter 2.1.4) for different amplitudes of the modulated magnetic field. We cannot determine the exact value of the modulated magnetic field amplitude until the spectra start to broaden. Thus, the modulated field amplitude for the first signal (upper spectrum in Fig. 6-1) is unknown. The following broadened signal (red curve) caused by over-modulation can be properly measured, which is convenient because the peak-to-peak width of the EPR signal equals to the amplitude of the over-modulated magnetic field [43].

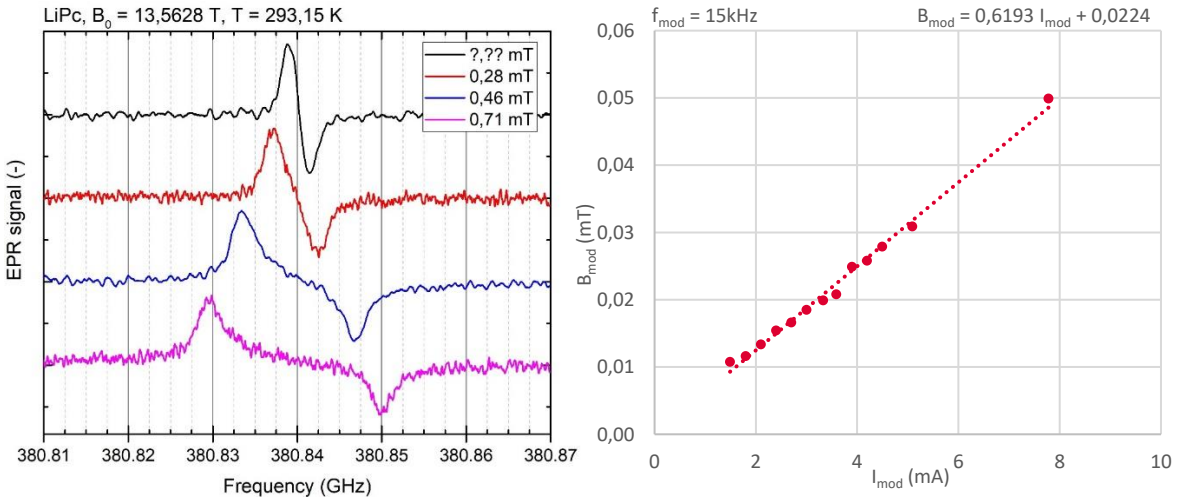

Fig. 6-1 EPR spectra obtained during modulation coil calibration and modulation amp.-current amp. dependence (LiPc - Pellet sample holder - CEITEC BUT).

Calculated modulation amplitudes can be fitted linearly with the amplitude of the alternating current flowing through the modulation coil. This process is repeated for several amplitudes of modulation, and data are processed into a graph and linear modulation-current dependencies. The linear approximations for several modulation frequencies for sample holder should be similar. It was not satisfactory for the chip sample holder, but the holder is still usable. Calibration data for each sample holder are included in attachments (see attachment A2, A3, and A4).

6.2 Measurement and design changes

Several design changes were performed during production to improve the functionality of the sample holders. The changes were required based on the experiences achieved during measurements. To reduce high production costs, all designed parts were produced in the workshop of CEITEC BUT.

6.2.1 Sample holder attachment

The universal flange was adjusted to use both systems, bayonet mechanism, and attachment by screws due to the inability to attach the chip sample holder caused by production inaccuracies. It allows us to attach also other devices that are not compatible with the bayonet mechanism.

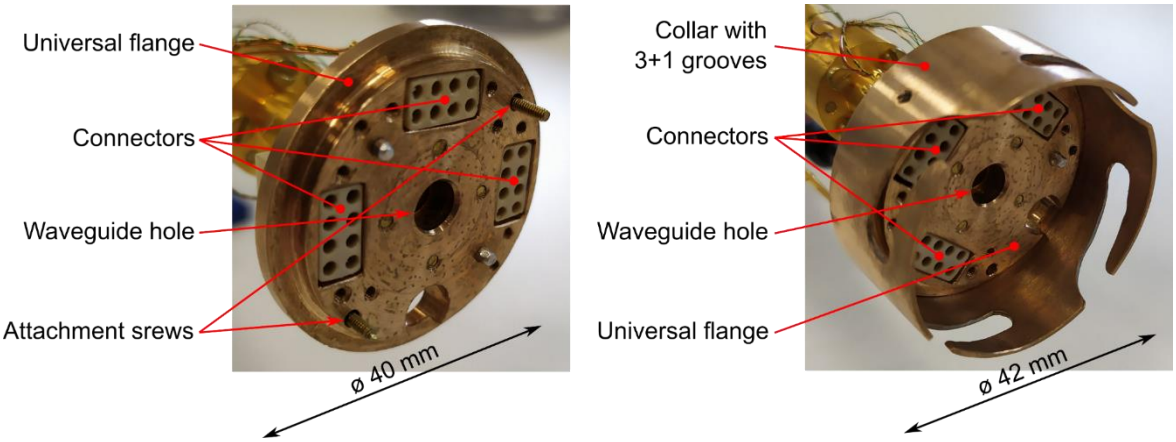

Fig. 6-2 Universal flange (left) with attachment with screws and bayonet mechanism (right), prototypes were produced in the workshop in CEITEC BUT.

6.2.2 Pellet sample holder

To improve the accuracy of the measured temperature in the area of the sample, the edge of the upper connector has been beveled. It allows us to attach the temperature sensor closer to the waveguide, which is in direct contact with the sample. All parts were made from PEEK ™ to test production quality and that was proven as very satisfying.

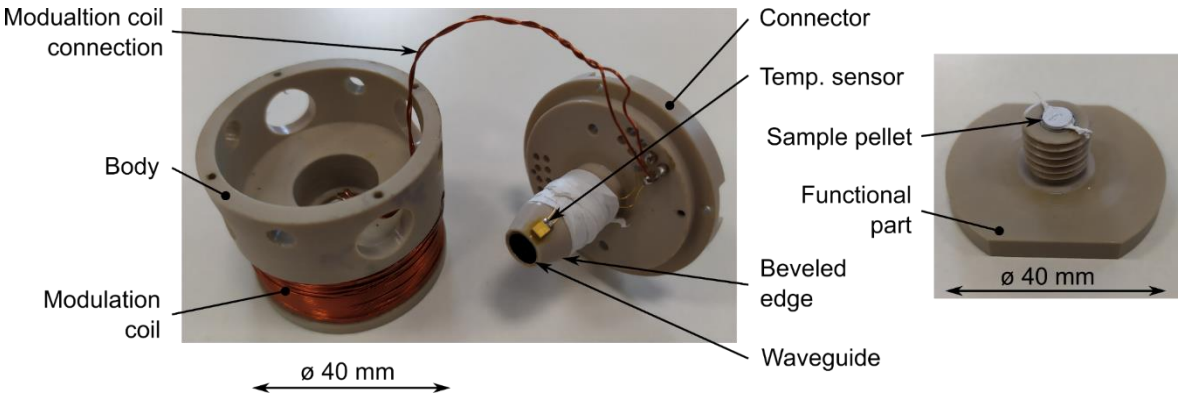

Fig. 6-3 Pellet sample holder prototype – disassembled – workshop CEITEC BUT.

6.2.3 Chip sample holder

The functionality of the sample holder was tested by modulation coil calibration but also on the few samples and devices including bolometers (see chapter 2.3.1 above). The first measurement of the bolometers was performed to find the most sensitive temperature area, where the bolometers can operate. The measurements (see Fig. 6-4) show the current-voltage dependence measured for several irradiation frequencies.

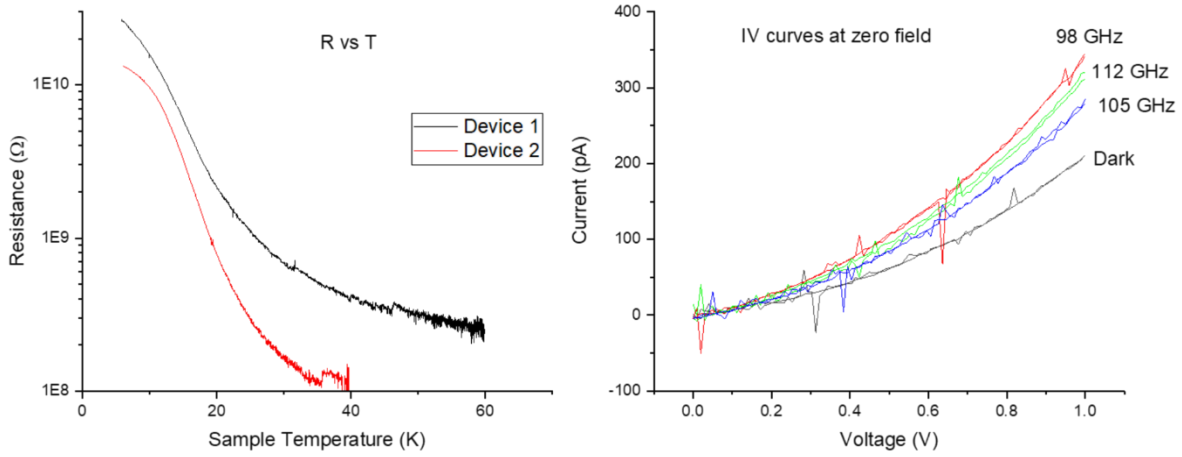

Fig. 6-4 Resistance-temperature dependence and current-voltage dependence for several irradiation frequencies – (Bolometer prepared by Luke St. Marie from Georgetown university – Chip sample holder – CEITEC BUT).

The production quality of Tufset as material for complicated parts is not completely satisfying (see Fig. 6-5). The inaccuracies created during the production of the prototype caused that the chip sample holder was not able to be attached by the bayonet mechanism.

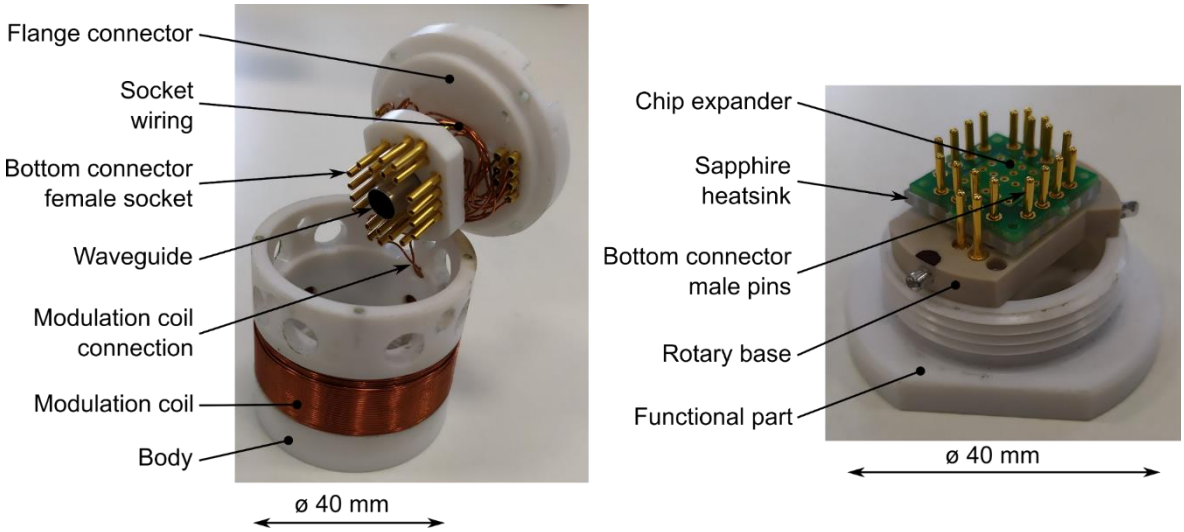

Fig. 6-5 Chip sample holder prototype – disassembled – workshop CEITEC BUT.

6.2.4 Carousel sample holder

The main problem of the design was that the position sensor was not able to work under the temperature of 70 K. This issue was solved by using the potentiometer as a source of the position information. It is provided by the measurement of the resistance of the potentiometer depending on the angle of rotation. The design uses already produced parts except for the Teflon® bearing, positioning plate, and the optical sensor.

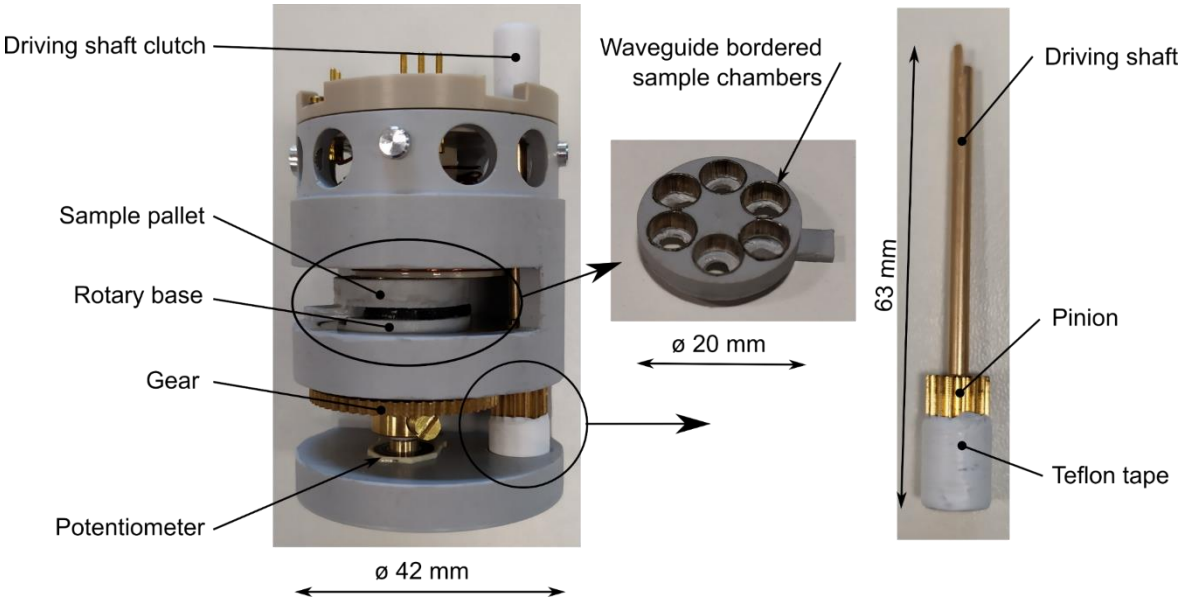

Fig. 6-6 Carousel sample holder prototype – assembled – workshop CEITEC BUT.

The irregular shape changes of Teflon® shrink tubes in low temperatures disabled the movement of the rotary base and other movable parts. This problem was resolved by the exclusion of the shrink tubes from the assembly and replacement by thinner Teflon® tape.

The sample platform was also adjusted. The fixation of the sample pellets via rings proved to be unreliable. The new design with sample chambers bordered with waveguide improved the irradiation propagation to the samples.

The pictures of the gearbox and probe shielding designed for the carousel sample holder is shown in the attachments (see attachment A6-4 and A6-5).

7 CONCLUSION

This bachelor thesis presents the design and manufacture of non-resonant sample holders for a high-field electron paramagnetic resonance (HF-EPR) spectrometer, proposed for powders pressed into pellets and samples deponed on the surface of a chip.

This work contains a brief theory of EPR spectroscopy, convenient for a basic understanding of the functionality of the HF-EPR spectrometer, and necessary for determining the construction requirements of sample holders. The concepts and construction of the universal flange, compatible with all developed sample holders and three concepts and designs of sample holders are also described. Pellet sample holder proposed to carry one pellet and chip sample holder, proposed to carry sample deponed on the chip expander, come out from the concept of bottom loading of the sample. Carousel sample holder comes from the concept of loading from the side and can carry up to 6 sample pellets in one loading. The work also contains the complete drawing documentation of holders designed for pellet sample form (carousel sample holder) and chip sample (chip sample holder).

As can be seen, the result of the work is the production of the universal attachment system and three sample holder prototypes, whose functionality was tested during modulation coil calibration, but also on other samples. The production of prototypes was performed in the workshop of the CEITEC BUT.

In the future, the design of sample holders could be adjusted for 3D print technology production. It would help to share the design for other scientific groups around the world.

8 BIBLIOGRAPHY

[1] BRUSTOLON, M., and E. GIAMELLO. *Electron Paramagnetic Resonance: A Practitioners Toolkit*. Hoboken (New Jersey): Wiley, 2008. ISBN 9780470258828.

[2] DUIN, E. Short introduction to Electron Paramagnetic Resonance. *Auburn University* [online]. Auburn (Alabama): Auburn University College of Sciences and Mathematics, ©2020 [accessed. 2020-01-27]. Available at: http://webhome.auburn.edu/~duinedu/epr/1_theory.pdf

[3] WEIL, J., and J.R. BOLTON. *Electron paramagnetic resonance: elementary theory and practical applications*. 2nd ed. Hoboken (New Jersey): Wiley, ©2007. ISBN 9780471754961.

[4] ODOM, B., D. HANNEKE, B. D'URSO, and G. GABRIELSE. New Measurement of the Electron Magnetic Moment Using and One-Electron Quantum Cyclotron. *Physical Review Letters* [online]. 2006, **97**(3), 3 [accessed. 2020-02-28]. DOI: 10.1103/PhysRevLett.97.030801. ISSN 0031-9007. Available at: https://link.aps.org/doi/10.1103/PhysRevLett.97.030801

[5] MOHR, P. J., D. B. NEWELL, and B. N. TAYLOR. CODATA recommended values of the fundamental physical constants: 2014. *Reviews of Modern Physics* [online]. 2016, **88**(3), 57 [accessed. 2020-02-28]. DOI: 10.1103/RevModPhys.88.035009. ISSN 0034-6861. Available at: https://link.aps.org/doi/10.1103/RevModPhys.88.035009

[6] WILLIAMS, E. R., R. L. STEINER, D. B. NEWELL, and P. T. OLSEN. Accurate Measurement of the Planck Constant. *Physical Review Letters* [online]. 1998, **81**(12), 2404-2407 [accessed. 2020-02-28]. DOI: 10.1103/PhysRevLett.81.2404. ISSN 0031-9007. Available at: https://link.aps.org/doi/10.1103/PhysRevLett.81.2404

[7] DRAGO, R. R. *Physical Methods for Chemists*. 2nd ed. Gainesville (Florida): Surfside Scientific Publishers, ©1977. ISBN 0030751764.

[8] KARUNAKARAN, CH., and M. BALAMURUGAN. *Spin Resonance Spectroscopy*. Amsterdam (Netherlands): Elsevier, 2018. ISBN 9780128136089.

[9] NEUGEBAUER, P. *Development of Heterodyne High Field / High Frequency Electron Paramagnetic Resonance Spectrometer at 285 GHz*. Grenoble (France), 2010. Ph.D. Thesis. Université Joseph-Fourier.

[10] Signal Generator Extension Modules. *Virginia Diodes, Inc - Your Source for Terahertz and mm-Wave Products* [online]. Charlottesville (Virginia): Virginia Diodes, ©2004-2020 [accessed. 2020-03-20]. Available at: https://vadiodes.com/en/products/signal-generator

[11] WEBER, R. T. *Xenon User's Guide: An EPR Primer*. Version 1.3. Billerica (Massachusetts): Bruker BioSpin Corporation The, ©2011.

[12] DAUSSY, C., M. GUINET, A. AMY-KLEIN, K. DJERROUD, Y. HERMIER, S. BRIAUDEAU, Ch. J. BORDÉ, and C. CHARDONNET. Direct Determination of the Boltzmann Constant by an Optical Method. *Physical Review Letters* [online]. 2007, **98**(25), 4 [accessed. 2020-02-29]. DOI: 10.1103/PhysRevLett.98.250801. ISSN 0031-9007. Available at: https://link.aps.org/doi/10.1103/PhysRevLett.98.250801

[13] NEUGEBAUER, P., D. BLOOS, R. MARX, et al. Ultra-broadband EPR spectroscopy in field and frequency domains. *Physical Chemistry Chemical Physics* [online]. 2018, **20**(22), 15528 [accessed. 2020-06-10]. DOI: 10.1039/C7CP07443C. ISSN 1463-9076. Available at: http://xlink.rsc.org/?DOI=C7CP07443C

[14] SOJKA, A. *Development of a Terahertz Magnetic Resonance Spectrometer for Electron Spin Dynamics Investigations*. Brno (Czech Republic), 2019. Ph.D. Thesis Topic. Brno University of Technology.

[15] MÖBIUS, K., and A. SAVITSKY. *High-field EPR spectroscopy on proteins and their model systems: characterization of transient paramagnetic states*. Cambridge: RSC Publishing, ©2009. ISBN 0854043683.

[16] REIJERSE, Edward J. High-Frequency EPR Instrumentation. *Applied Magnetic Resonance* [online]. 2010, **37**(1-4), 802-807 [accessed. 2020-05-20]. DOI: 10.1007/s00723-009-0070-y. ISSN 09379347. Available at: http://link.springer.com/10.1007/s00723-009-0070-y

[17] PHILLIPS, J. C. Bonding, and Structure in Solids. MEYERS, R. A., ed. *Encyclopedia of Physical Science and Technology*. 3rd ed. Elsevier, ©2001, s. 301. ISBN 9780122274107.

[18] EL FATIMY, A., P. HAN, N. QUIRK, et al. Effect of defect-induced cooling on graphene hot-electron bolometers. *Carbon* [online]. 2019, **154**, 497-502 [accessed. 2020-06-20]. DOI: 10.1016/j.carbon.2019.08.019. ISSN 00086223. Available at: https://linkinghub.elsevier.com/retrieve/pii/S0008622319308164

[19] HESLER, J. L., L. LIUB, H. XUB, Y. DUANA, and R. M. WEIKLEB. The Development of Quasi-Optical THz Detectors. *Virginia Diodes, Inc - Your Source for Terahertz and mm-Wave Products* [online]. Charlottesville (Virginia): Virginia Diodes, ©2004-2020 [accessed. 2020-03-20]. Available at: https://www.vadiodes.com/images/pdfs/HeslerQuasiOpticalDetectors.pdf

[20] GOLDSMITH, P. F. *Quasioptical systems: Gaussian beam quasioptical propagation and applications*. Piscataway (New Jersey): IEEE Press, [1998]. IEEE Press. ISBN 9780780334397.

[21] BLOK, H. *Electron Paramagnetic Resonance and Electron Nuclear Double Resonance Spectroscopy at 275 GHz*. Leiden, 2006. Ph.D. Thesis. Universiteit van Leiden.

[22] Cryogen Free Magnet System 9-18 Tesla (CFMS). *Cryogenic Limited* [online]. London (United Kingdom): Cryogenic Limited, ©2020 [accessed. 2020-03-12]. Available at: https://www.cryogenic.co.uk/products/cryogen-free-magnet-system-9-18-tesla-cfms

[23] MOLINARI, Vincenzo, Domiziano MOSTACCI, and Barry D. GANAPOL. The Specific Heat of Liquid Helium. *Journal of Computational and Theoretical Transport* [online]. 2016, **45**(3), 217 [accessed. 2020-02-29]. DOI: 10.1080/23324309.2016.1156549. ISSN 2332-4309. Available at: https://www.tandfonline.com/doi/full/10.1080/23324309.2016.1156549

[24] WEBER, R. T., J. J. JIANG, and D. P. BARR. *EMX User's Manual: Removing and Inserting Samples*. Version 2.0. Billerica (Massachusetts): Bruker Instruments, ©1998.

[25] CLARKE, R. N., and C. B. ROSENBERG. Fabry-Perot and open resonators at microwave and millimetre wave frequencies, 2-300 GHz. *Journal of Physics E: Scientific Instruments* [online]. 1982, **15**(1), 19 [accessed. 2020-03-20]. DOI: 10.1088/0022-3735/15/1/002. ISSN 00223735. Available at: https://iopscience.iop.org/article/10.1088/0022-3735/15/1/002

[26] VAN TOL, J., L.-C. BRUNEL and R. J. WYLDE. A quasioptical transient electron spin resonance spectrometer operating at 120 and 240 GHz. *Review of Scientific Instruments* [online]. 2005, **76**(7), 4 [accessed. 2020-06-19]. DOI: 10.1063/1.1942533. ISSN 00346748. Available at: http://aip.scitation.org/doi/10.1063/1.1942533

[27] STOLL, R. L. *The analysis of eddy currents*. London (United Kingdom): Oxford University Press, ©1974. ISBN 0198593112.

[28] Helmholtz Coils. *University of Wisconsin–Madison* [online]. Madison (Wisconsin): University of Wisconsin, ©2020 [accessed. 2020-06-19]. Available at: https://wp.physics.wisc.edu/ingersollmuseum/exhibits/em/helmholtz/

[29] HEANEY, M. B. Electrical Conductivity and Resistivity. WEBSTER, J. G., ed. *Electrical Measurement, Signal Processing, and Displays*. Boca Raton (Florida): CRC Press, 2003, 7-4 - 7-5. ISBN 9780849317330.

[30] Cryogenic Wire. *Lake Shore Cryotronics, Inc* [online]. Westerville (Ohio): Lake Shore Cryotronics, ©2019 [accessed. 2020-04-06]. Available at: https://www.lakeshore.com/products/categories/specification/temperature-products/cryogenic-accessories/cryogenic-wire

[31] Alloy - Electrical Properties. *Supplier of materials for research and development - Goodfellow* [online]. Cambridge (United Kingdom): Goodfellow, ©2008-2020 [accessed. 2020-04-06]. Available at: http://www.goodfellow.com/PDF/TAB011X.pdf

[32] Water Absorption 24 Hour - (ASTM D570) Test of Plastics. *Plastic Materials | Free Online Database for Plastic Industry* [online]. Paris (France): SpecialChem, ©2020 [accessed. 2020-04-06]. Available at: https://omnexus.specialchem.com/polymer-properties/properties/water-absorption-24-hours

[33] Polyether ether ketone (PEEK Plastic): Uses, Properties & Material Guide. *Plastic Materials | Free Online Database for Plastic Industry* [online]. Paris (France): SpecialChem, ©2020 [accessed. 2020-04-06]. Available at: https://omnexus.specialchem.com/selection-guide/polyetheretherketone-peek-thermoplastic

[34] Pins & Sockets for C & D Connectors. *LewVac Components Ltd | Manufacturer of Vacuum Components* [online]. Burgess Hill (United Kingdom): LewVac Components Limited, ©2018 [accessed. 2020-04-07]. Available at: https://www.lewvac.co.uk/product/pins-sockets-for-c-d-connectors/

[35] Wiring Tools etc. *LewVac Components Ltd | Manufacturer of Vacuum Components* [online]. Burgess Hill (United Kingdom): LewVac Components Limited, ©2018 [accessed. 2020-04-07]. Available at: https://www.lewvac.co.uk/product/wiring-tools-etc/

[36] Tufnol tufset | Abrasive disc backing | ERBGF | Fabric Laminates | Plastic machining components. *Tufnol, Engineering plastics, and composites...* [online]. Birmingham (United Kingdom): Tufnol Composites, ©2020 [accessed. 2020-06-24]. Available at: https://tufnol.com/materials-full/themoplastics/tufnol-tufset.aspx

[37] DOBROVINSKAYA, E. R., L. A. LYTVYNOV, and V. PISHCHIK. *Sapphire: Material, Manufacturing, Applications*. New York (USA): Springer, ©2009. ISBN 9780387856940.

[38] GAITONDE, J.M., and M.V. LOWSON. Low-temperature thermal expansion of PEEK, HTA, and some of their composites reinforced with carbon fibres. *Composites Science and Technology* [online]. 1991, **40**(1), 70-76 [accessed. 2020-04-07]. DOI: 10.1016/0266-3538(91)90043-O. ISSN 02663538. Available at: https://linkinghub.elsevier.com/retrieve/pii/026635389190043O

[39] KIA, H. G. Thermal expansion of polyurethane reinforced with continuous glass fibers. *Polymer Composites* [online]. 1988, **9**(3), 239 [accessed. 2020-04-07]. DOI: 10.1002/pc.750090311. ISSN 0272-8397. Available at: http://doi.wiley.com/10.1002/pc.750090311

[40] KIRBY, R. K. Thermal expansion of polytetrafluoroethylene (Teflon) from -190 to +300 C. *Journal of Research of the National Bureau of Standards* [online]. 1956, **57**(2), 92-94 [accessed. 2020-04-07]. DOI: 10.6028/jres.057.010. ISSN 0091-0635. Available at: https://nvlpubs.nist.gov/nistpubs/jres/057/jresv57n2p91_A1b.pdf

[41] EE-SX1320. *Omron Electronic Components Europe - A global leader in the field of automation* [online]. Kyoto (Japan): Omron Corporation, ©2020 [accessed. 2020-06-24]. Available at: http://components.omron.eu/Product-details/EE-SX1320

[42] LEGS Rotary LR23-50. *PiezoMotor* [online]. Uppsala (Sweden): PiezoMotor, ©2017-2020 [accessed. 2020-06-24]. Available at: https://piezomotor.com/legs-rotary-lr23-50/

[43] JIANG, J. J., and R. T. WEBER. *Elexsys E 500 User's Manual: Advanced Operations: EPR Spectrometer Calibration*. Version 1.0. Billerica (Massachusetts): Bruker BioSpin Corporation, ©2001.

9 LIST OF ABBREVIATIONS, SYMBOLS AND PHYSICAL VALUES

Used abbreviations:

EPR	Electron paramagnetic resonance
ESR	Electron spin resonance
HF-EPR	High-field electron paramagnetic resonance
MW	Microwave
VTI	Variable temperature insert
PEEK	Polyether-ether-ketone
PU	Polyurethane
PTFE	Polytetrafluoroethylene

Used physical values and constants:

$\vec{S}, S, S_z$	Electron spin angular momentum, its magnitude and z component
s	Electron spin quantum number
$\vec{\mu}_e$	Electron magnetic moment
g	Landé factor (g factor)
μ_B	Bohr magneton
$E, E_{\alpha,\beta}, \Delta E$	Energy, the energy of α and β state, the energy difference
$\vec{B}, B_0$	Magnetic field and its intensity
h	Planck's constant
$\mathcal{H}, \mathcal{H}_{XY}$	Spin Hamiltonian and its components
N_α, N_β	Population of electrons in α and β state
ν	Radiation frequency
k_B	Boltzmann constant
T	Thermodynamic temperature

10 LIST OF FIGURES

11 LIST OF TABLES

12 LIST OF ATTACHMENTS

Included attachments:

A1 – Probe wiring connection

A2 – Pellet sample holder – Datasheet

A3 – Chip sample holder – Datasheet

A4 – Carousel sample holder – Datasheet

A5 – Carousel sample holder dimension tolerances calculation

A6 – Photo documentation

Separated attachments:

A7 – Drawings – Chip sample holder

A8 – Drawings – Carousel sample holder

13 ATTACHMENTS

A1 – Probe wiring connection

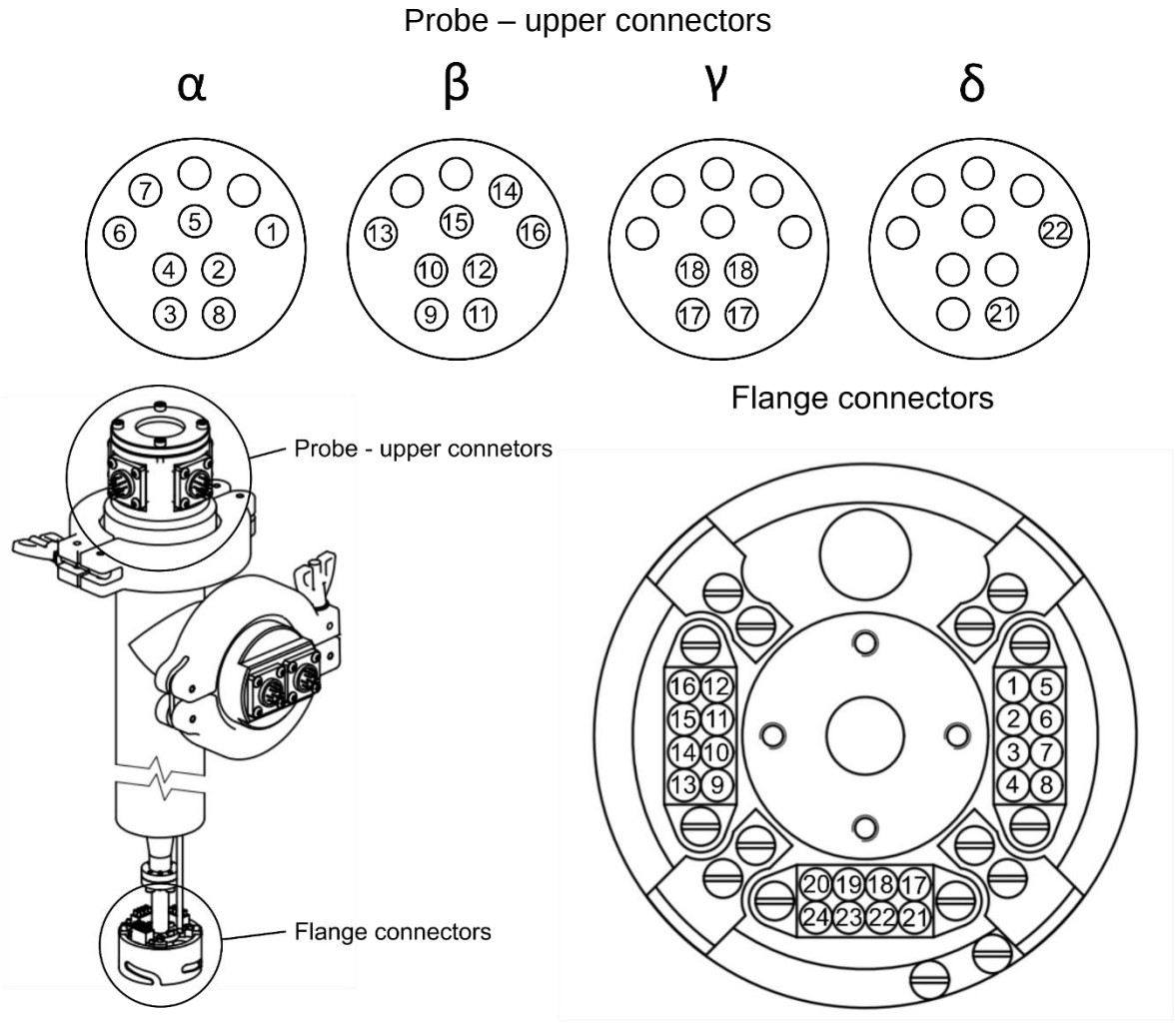

No.	Wire	R (Ω)	No.	Wire	R (Ω)	No.	Wire	R (Ω)
1	NiCr 32 AWG	56.3	**9**	NiCr 32 AWG	42.8	**17**	Cu 26 AWG	4-point method
2	NiCr 32 AWG	58.2	**10**	NiCr 32 AWG	47	**18**	Cu 26 AWG	4-point method
3	NiCr 32 AWG	56.7	**11**	NiCr 32 AWG	47.4	**19**	Cu 26 AWG	not necessary
4	NiCr 32 AWG	56.7	**12**	NiCr 32 AWG	47.4	**20**	Cu 26 AWG	not necessary
5	NiCr 32 AWG	56.5	**13**	NiCr 32 AWG	47.8	**21**	Cu 26 AWG	not necessary
6	NiCr 32 AWG	56.6	**14**	NiCr 32 AWG	47.3	**22**	Cu 26 AWG	not necessary
7	NiCr 32 AWG	56.6	**15**	NiCr 32 AWG	47.7	**23**	reserve	-
8	NiCr 32 AWG	56.5	**16**	NiCr 32 AWG	47.8	**24**	reserve	-

T = 20°C, State in date: 01.05.2020

A2 – Pellet sample holder – datasheet

Modulation coil calibration

Measurement conditions:
Sample: LiPc (Lithium Phthalocyanine)
Frequency sweep: 380.77-380.87 GHz
Magnetic field: 13.563 T

Modulation coil properties:
Wire type: Cu 26 AWG – Kapton® insulation
Wire turns: 532
Dimensions:

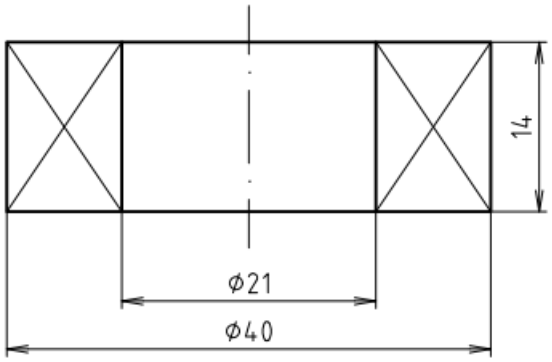

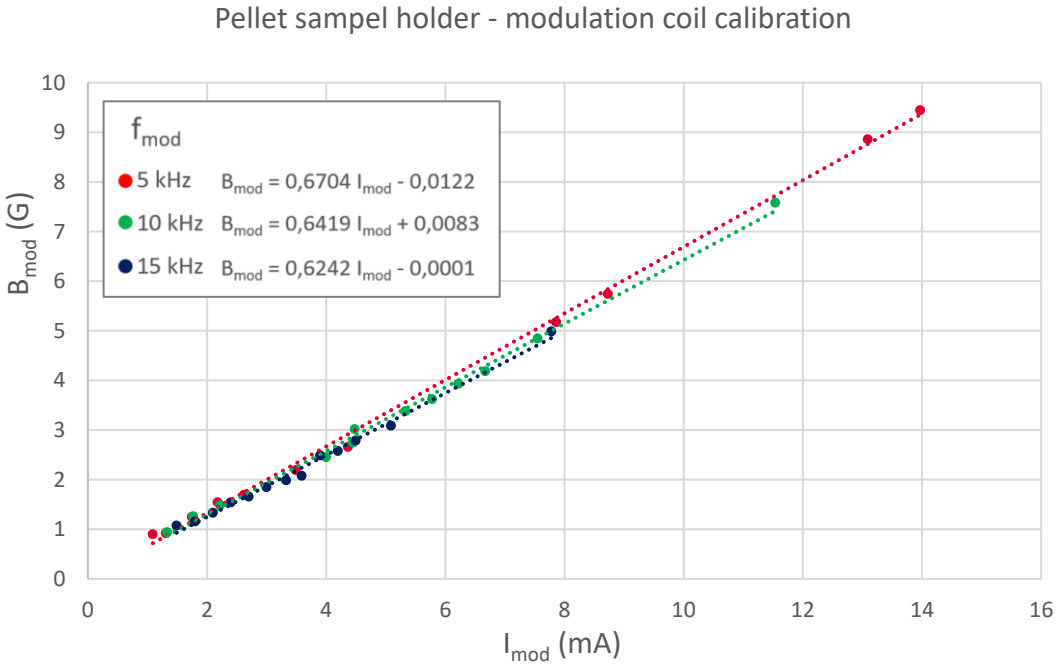

Wiring connection

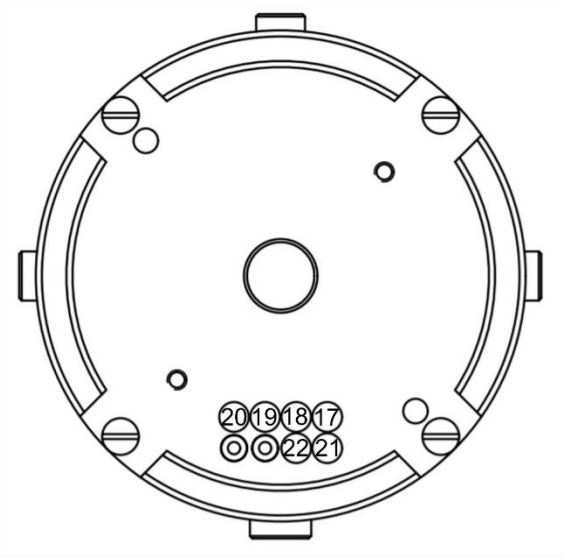

No.	Device
17	Temperature sensor
18	Temperature sensor
19	Heater
20	Heater
21	Modulation coil
22	Modulation coil

A3 – Chip sample holder – datasheet

Modulation coil calibration:

Measurement conditions:
Sample: LiPc (Lithium Phthalocyanine)
Frequency sweep: 102.5-103 GHz
Magnetic field: 3.7 T

Modulation coil properties:
Wire type: Cu 26 AWG – Kapton® insulation
Wire turns: 300
Dimensions:

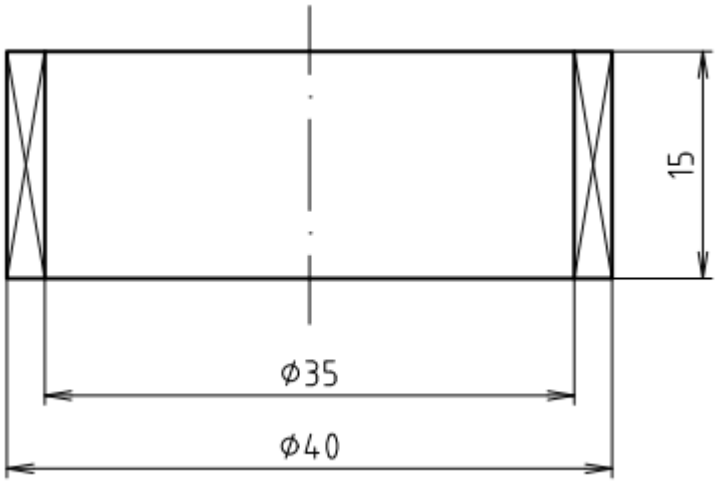

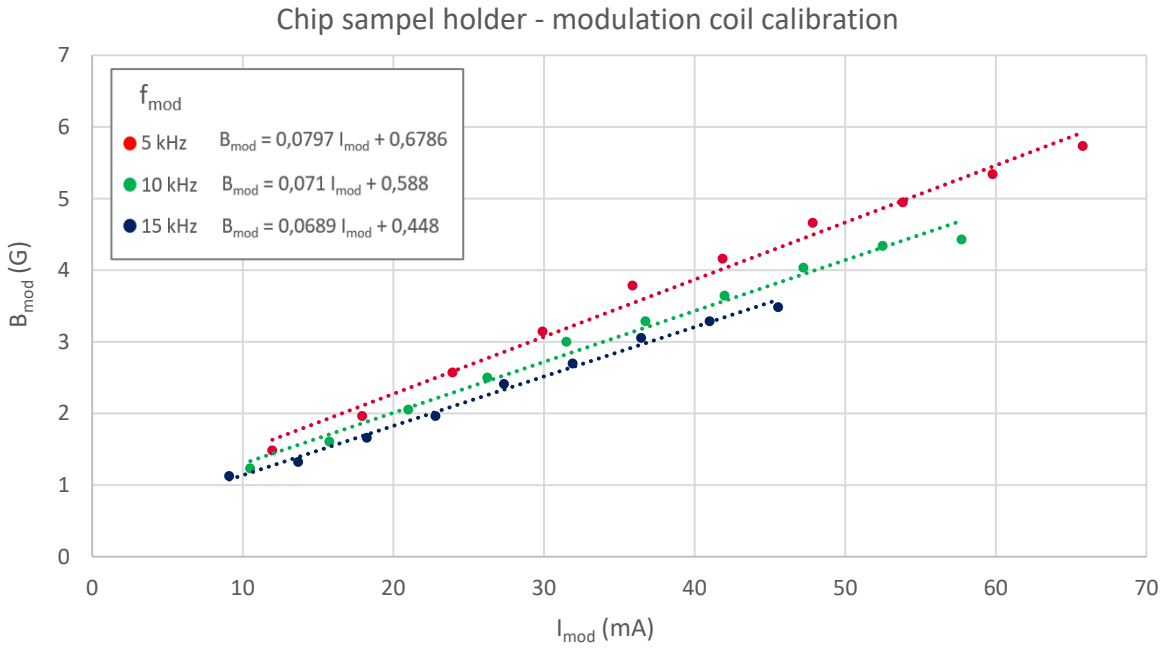

Wiring connection:

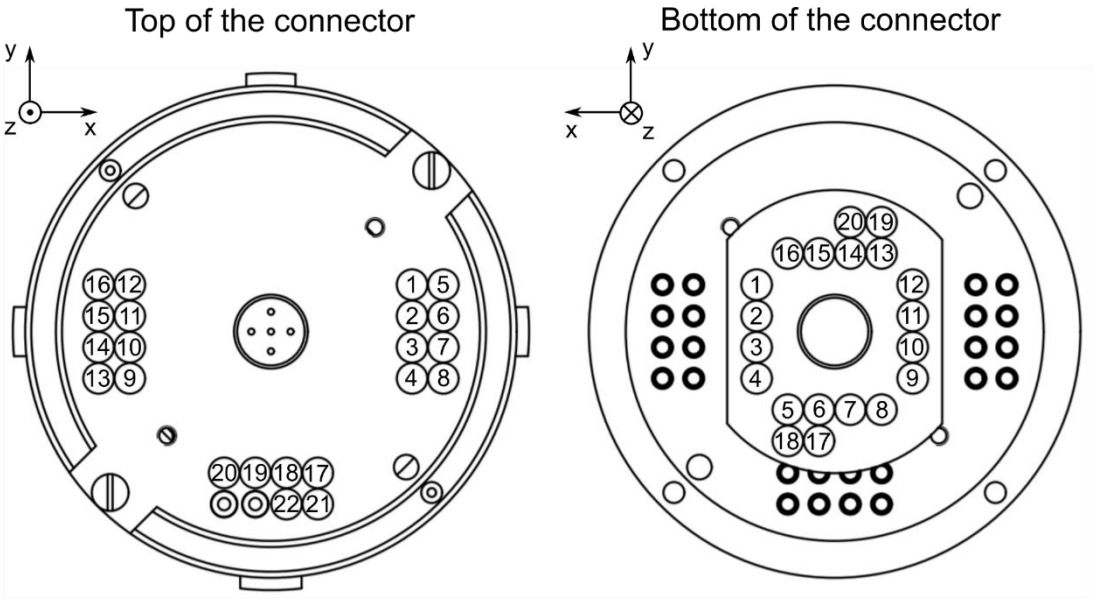

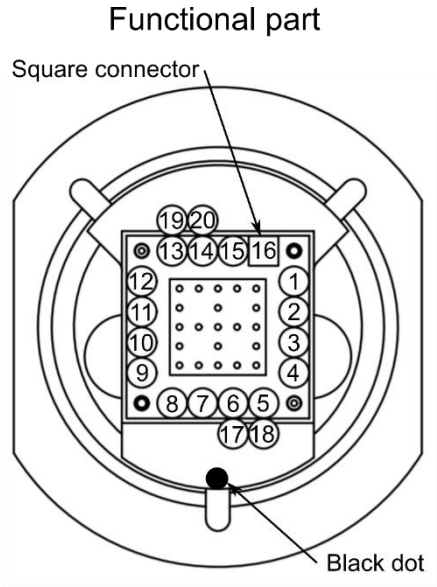

No.	Device	No.	Device	No.	Device	No.	Device
1	Chip expander	**7**	Chip expander	**13**	Chip expander	**19**	Heater
2	Chip expander	**8**	Chip expander	**14**	Chip expander	**20**	Heater
3	Chip expander	**9**	Chip expander	**15**	Chip expander	**21**	Modulation coil
4	Chip expander	**10**	Chip expander	**16**	Chip expander	**22**	Modulation coil
5	Chip expander	**11**	Chip expander	**17**	Temp. sensor		
6	Chip expander	**12**	Chip expander	**18**	Temp. sensor		

A4 – Carousel sample holder – datasheet

Modulation coil calibration:

Measurement conditions:
Sample: LiPc (Lithium Phthalocyanine)
Frequency sweep: 202.3-202.7 GHz
Magnetic field: 7.277 T

Modulation coil properties:
Wire type: Cu 26 AWG – Kapton® insulation
Wire turns: 168
Dimensions:

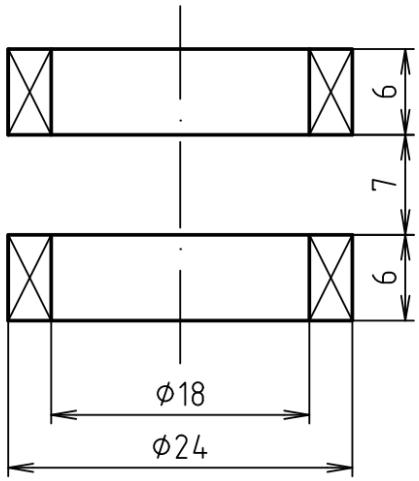

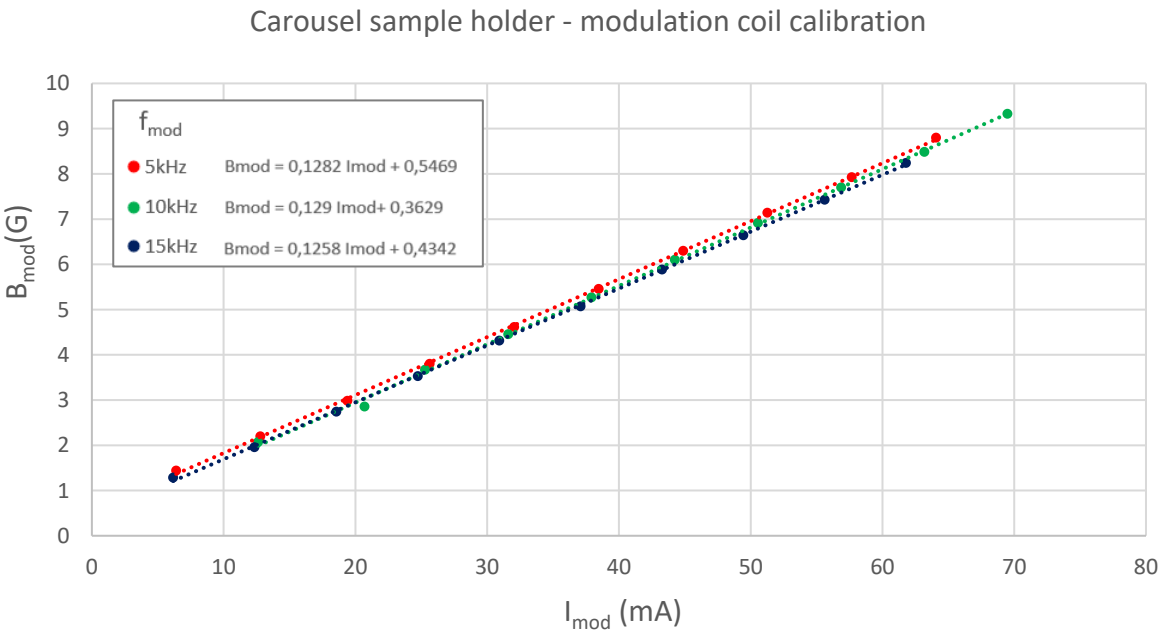

Wiring connection

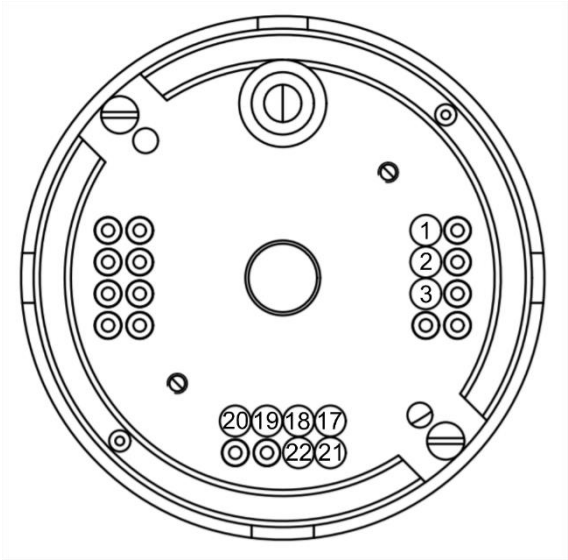

No.	Device	No.	Device
1	Potentiometer	**19**	Heater
2	Potentiometer – middle conductor	**20**	Heater
3	Potentiometer	**21**	Modulation coil
17	Temperature sensor	**22**	Modulation coil
18	Temperature sensor		

A5 – carousel sample holder dimension tolerances calculation

Scheme 1

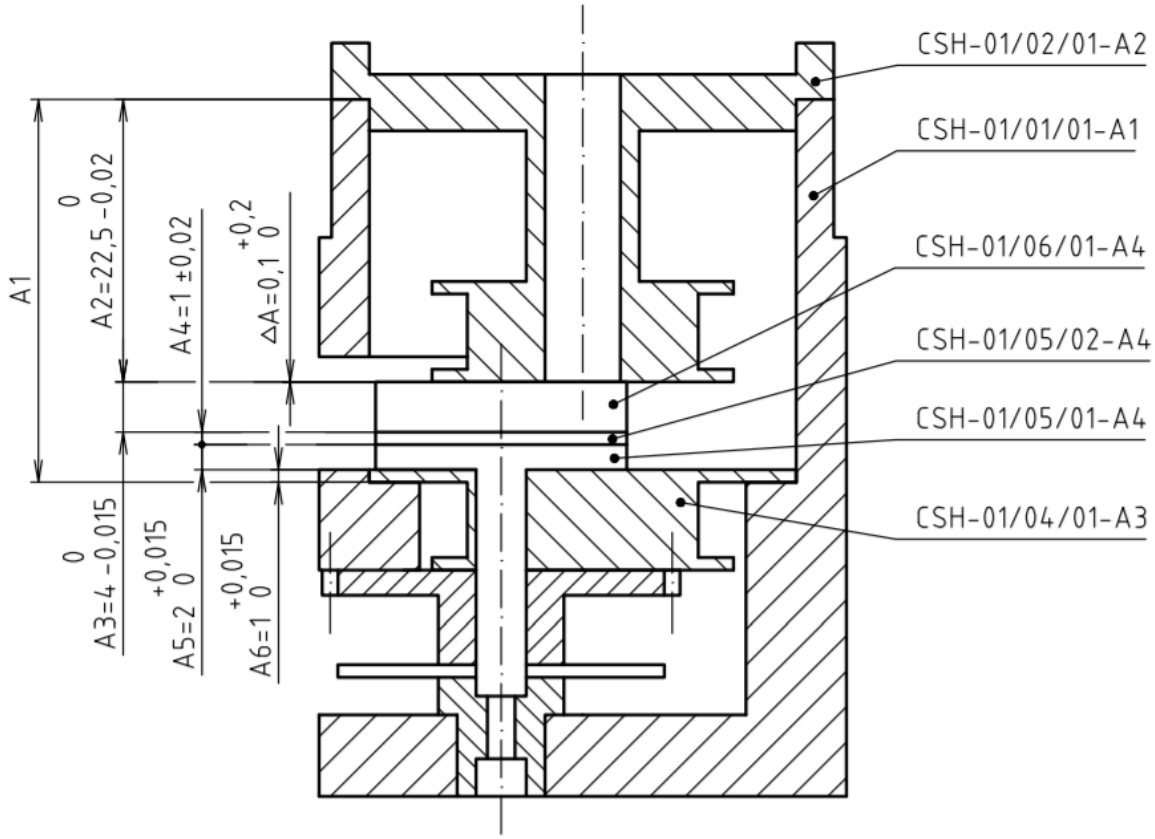

Nominal dim.:	Upper limits:	Lower limits:	Tolerance field:
$A_{\Delta nom} := 0.1\ mm$	$A_{\Delta max} := 0.3\ mm$	$A_{\Delta min} := 0.1\ mm$	$T_{\Delta} := A_{\Delta max} - A_{\Delta min} = 0.2\ mm$
$A_{2nom} := 22.5\ mm$	$A_{2max} := 22.5\ mm$	$A_{2min} := 22.48\ mm$	$T_2 := A_{2max} - A_{2min} = 0.02\ mm$
$A_{3nom} := 4\ mm$	$A_{3max} := 4\ mm$	$A_{3min} := 3.985\ mm$	$T_3 := A_{3max} - A_{3min} = 0.015\ mm$
$A_{4nom} := 1\ mm$	$A_{4max} := 1.02\ mm$	$A_{4min} := 0.98\ mm$	$T_4 := A_{4max} - A_{4min} = 0.04\ mm$
$A_{5nom} := 2\ mm$	$A_{5max} := 2.015\ mm$	$A_{5min} := 2\ mm$	$T_5 := A_{5max} - A_{5min} = 0.015\ mm$
$A_{6nom} := 1\ mm$	$A_{6max} := 1.015\ mm$	$A_{6min} := 1\ mm$	$T_6 := A_{6max} - A_{6min} = 0.015\ mm$

Verification of the realization:

$$T_1 := T_{\Delta} - T_2 - T_3 - T_4 - T_5 - T_6 = 0.095\ mm$$

Lower limit:

$$A_{1min} := A_{\Delta min} + A_{2max} + A_{3max} + A_{4max} + A_{5max} + A_{6max} = 30.65\ mm$$

Upper limit:

$$A_{1max} := A_{\Delta max} + A_{2min} + A_{3min} + A_{4min} + A_{5min} + A_{6min} = 30.745\ mm$$

Scheme 2

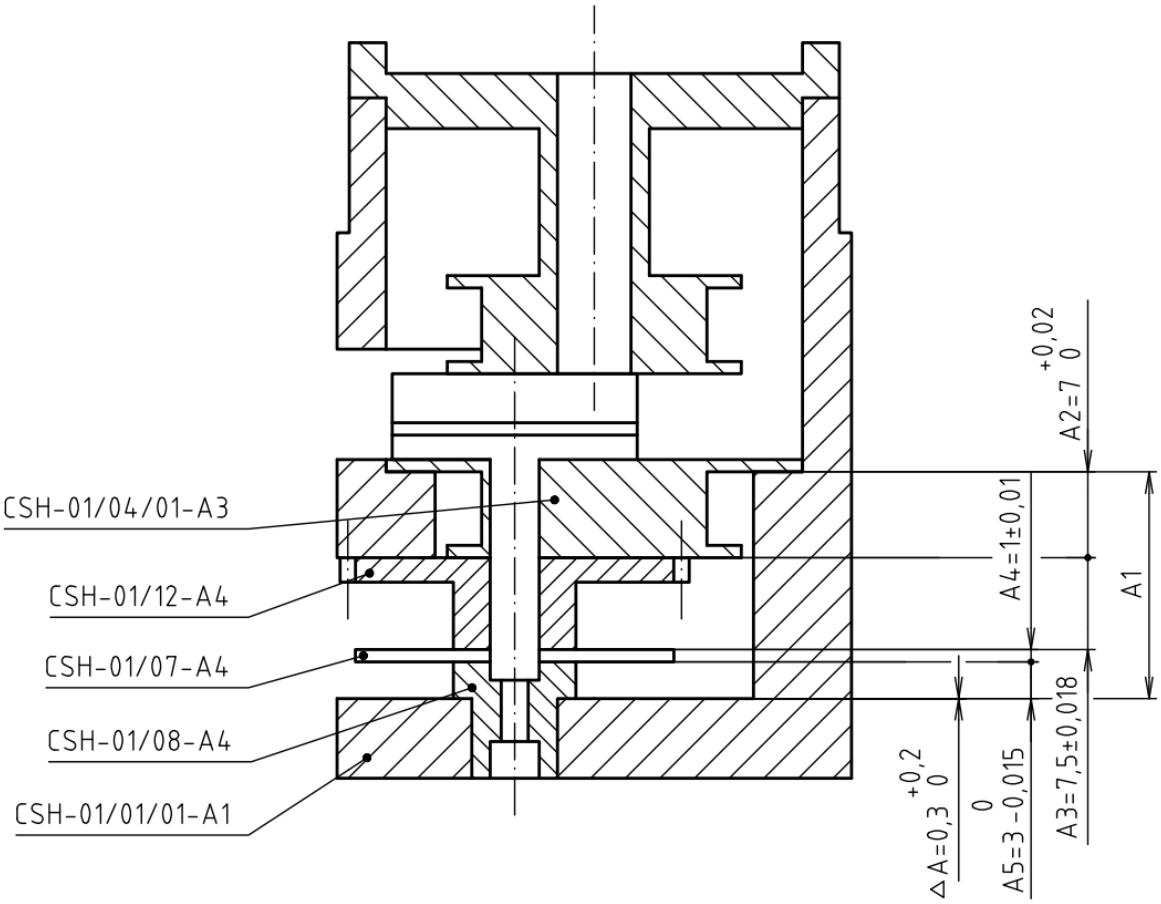

Nominal dim.:	Upper limits:	Lower limits:	Tolerance field:
$A_{\Delta nom} := 0.3$ mm	$A_{\Delta max} := 0.5$ mm	$A_{\Delta min} := 0.3$ mm	$T_\Delta := A_{\Delta max} - A_{\Delta min} = 0.2$ mm
$A_{2nom} := 7$ mm	$A_{2max} := 7.02$ mm	$A_{2min} := 7$ mm	$T_2 := A_{2max} - A_{2min} = 0.02$ mm
$A_{3nom} := 7.5$ mm	$A_{3max} := 7.518$ mm	$A_{3min} := 7.482$ mm	$T_3 := A_{3max} - A_{3min} = 0.036$ mm
$A_{4nom} := 1$ mm	$A_{4max} := 1.01$ mm	$A_{4min} := 0.99$ mm	$T_4 := A_{4max} - A_{4min} = 0.02$ mm
$A_{5nom} := 3$ mm	$A_{5max} := 3$ mm	$A_{5min} := 2.985$ mm	$T_5 := A_{5max} - A_{5min} = 0.015$ mm

Verification of the realization:

$$T_1 := T_\Delta - T_2 - T_3 - T_4 - T_5 = 0.109 \text{ mm}$$

Lower limit:

$$A_{1min} := A_{\Delta min} + A_{2max} + A_{3max} + A_{4max} + A_{5max} = 18.848 \text{ mm}$$

Upper limit:

$$A_{1max} := A_{\Delta max} + A_{2min} + A_{3min} + A_{4min} + A_{5min} = 18.957 \text{ mm}$$

A6 – Photo documentation

A6-1 – HF-EPR spectrometer – CEITEC BUT in Brno

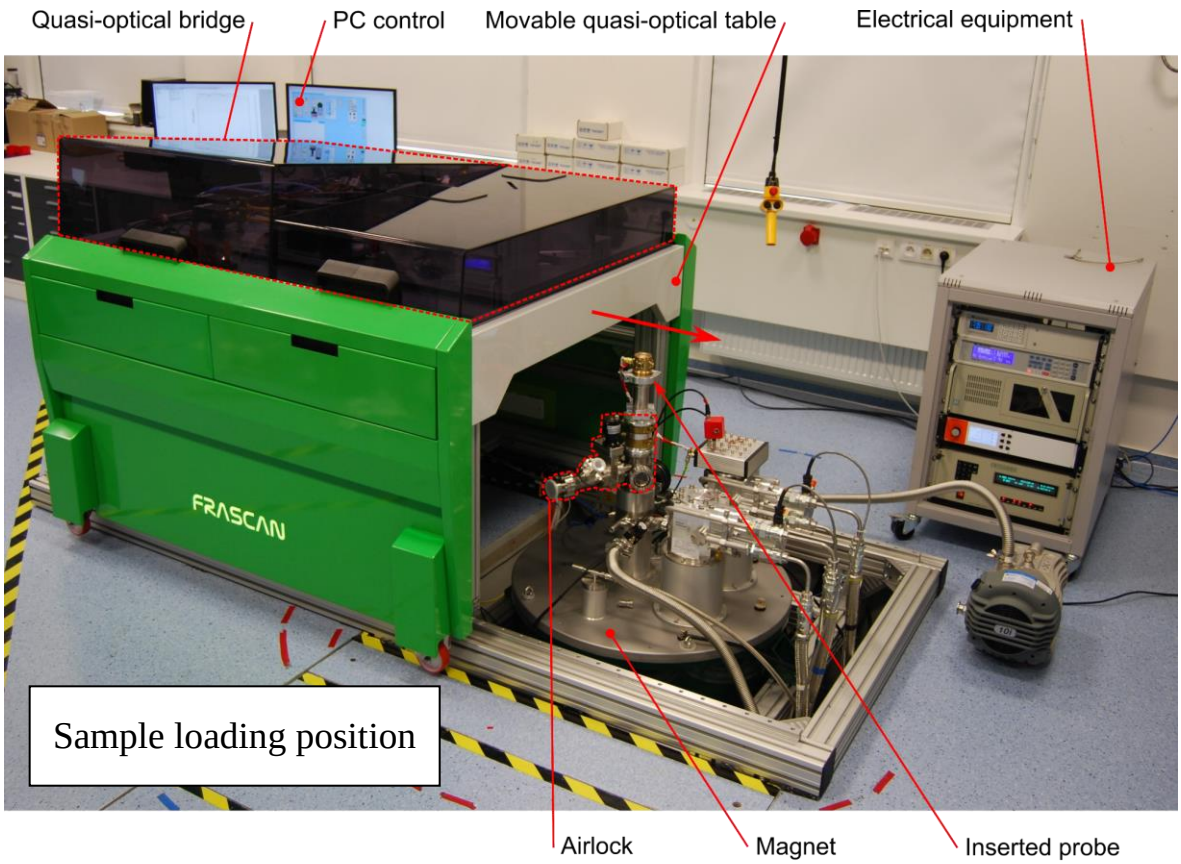

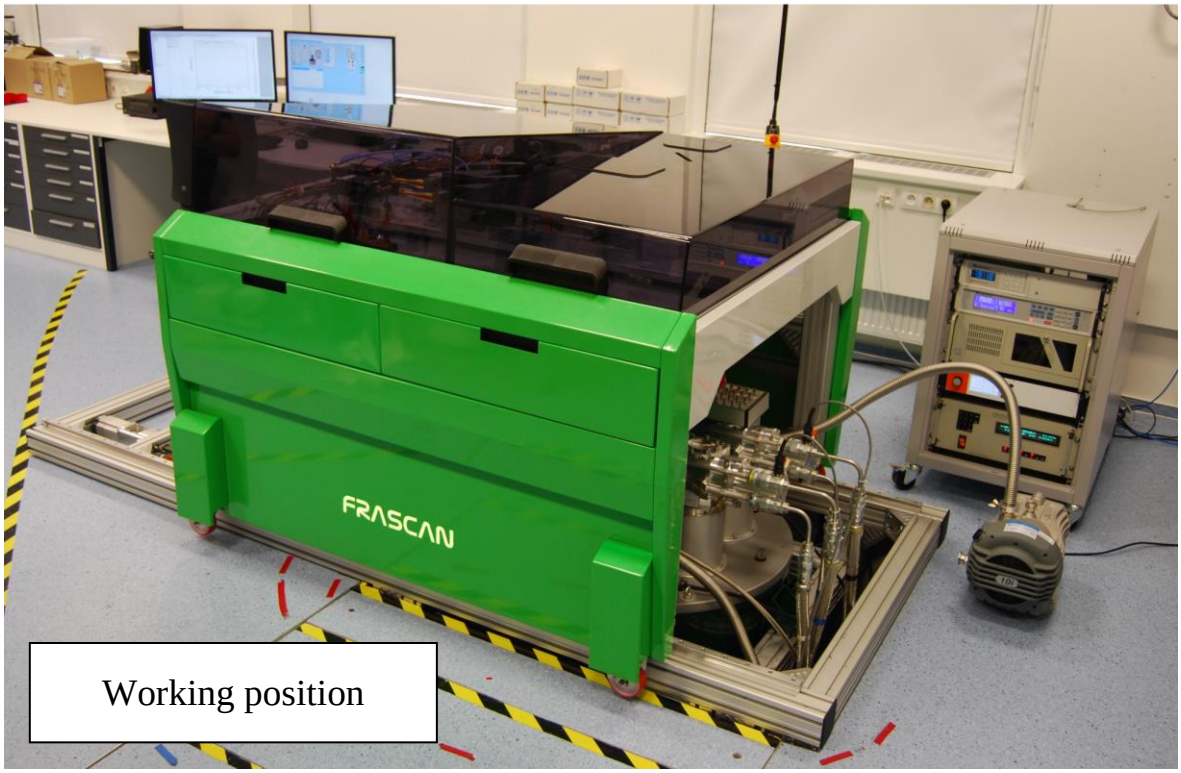

A6-2 – Ejected probe

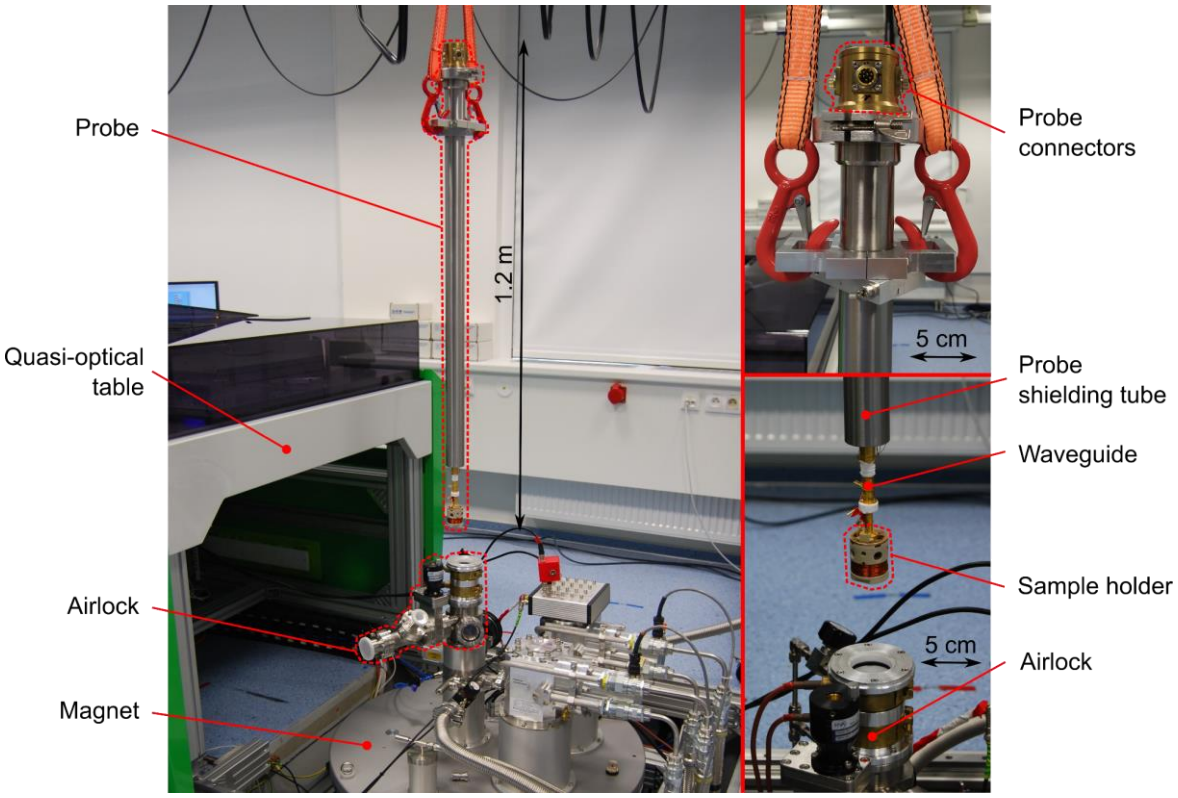

A6-3 – Bayonet mechanism – sample holder insertion

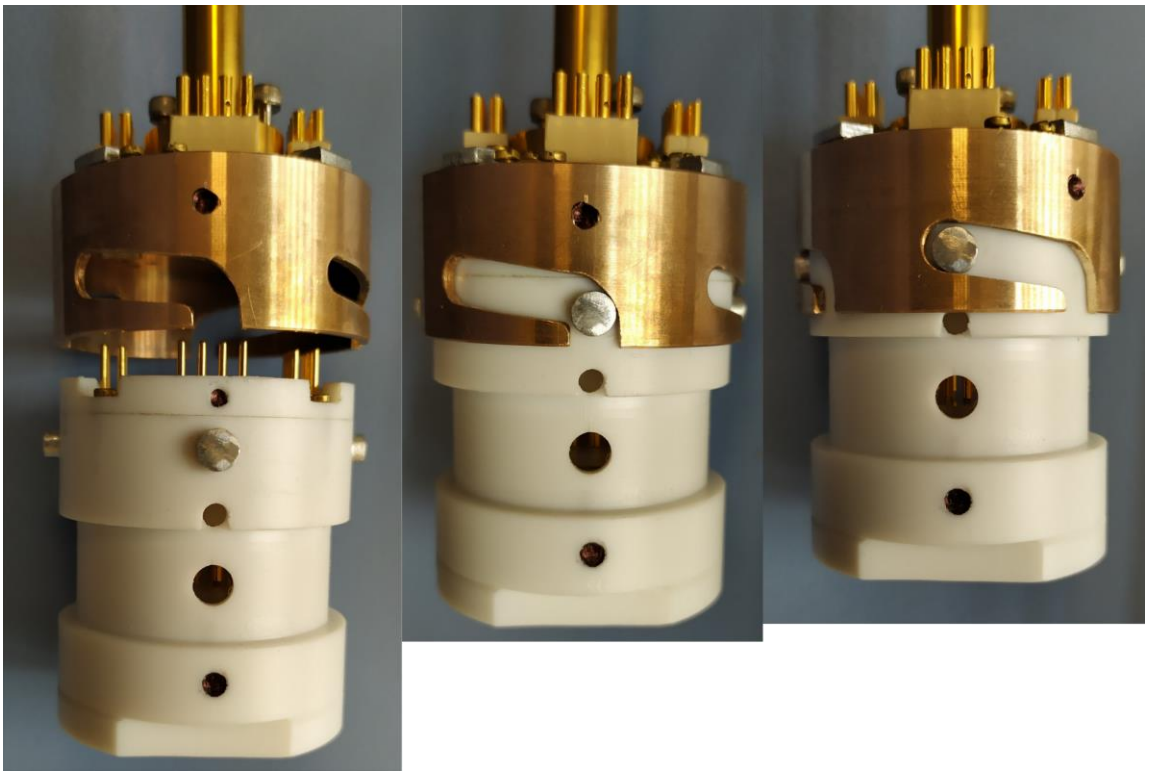

A6-4 – Probe shielding adjustment

A6-5 – Gearbox – detailed view